Technology Report

Optical Wireless Communications in Space

Luis Enrique García Muñoz

Pablo Fajardo Peña

uc3m | Universidad Carlos III de Madrid

Content

1. Introduction

To date, communications in space between spacecraft and mission control have preferentially used radio-frequency (RF) standards, with on-board radios for data transmission and navigation needs. The preferred frequency bands are the S-band (1.7 to 2.7 GHz), Ku-band (10.6 to 15.7 GHz) and Ka-band (17.3 to 31 GHz), using highly complex modulation/demodulation architectures to achieve high data rates within these limited channel bandwidths. This has led to the development of global networks, comprised of ground stations and space-based relay satellites, which have expanded over the last years, drastically improving space communication services.

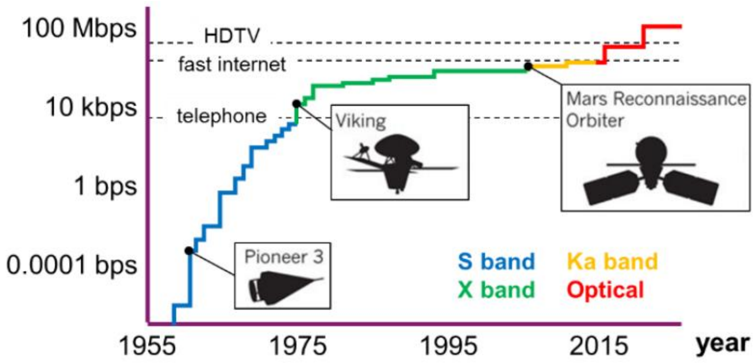

Figure 1: Interplanetary data transmission rates increase over time as higher frequency bands of radio waves are accessed [1].

As shown in **Figure 1**, the data rates of space missions have increased by ten orders of magnitude in the past 50 years. This motivated the increase in radio communication carrier frequency, moving away from lower bands which suffer from limited channel capacity and transmission rate due to the limited radio spectrum available. While today's mission communication requirements have begun to stress the current communication networks' capabilities, it has become clear that the communication services for future missions are demanding higher and faster data rates. The search for more capable and effective solutions for future space communication has begun.

A straightforward solution is to increase the carrier wave frequency, making new bands of the spectrum available at atmospheric attenuation minima, shown in Figure 2. One solution is to move into the millimetre- (MMW, 30 GHz to 300 GHz) and Terahertz (THz, 300 GHz to 3 THz) waves for ultrahigh-speed wireless links. An alternative to this, are Optical Wireless Communication (OWC), which emerged as an alternative to millimetre-wave to meet the increasing demand for high data rate services. OWC operates at optical frequencies, both in the Infrared (Infrared communications, IRC) and visible (Visible Light Communications, VLC) spectrum regions, vast amounts of bandwidth are readily available.

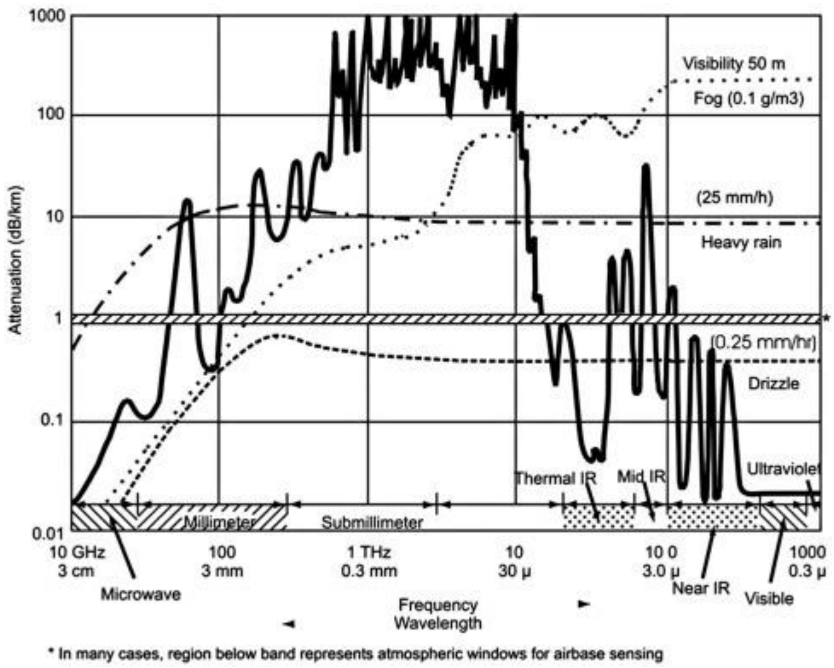

Figure 2: *Atmospheric attenuation in the electromagnetic spectrum.*

Unlike radio wave communications, optical communication systems in space can make their antennas compact. Taking advantage of the wide modulation bandwidth characteristics of lasers, lightweight compact communication equipment mounted on a satellite can realize high-speed large-capacity communications.

Optical communications have attracted attention as a next-generation technology for space communication networks using satellites. However there are particular technologies for this scenario, such as high-precision tracking and pointing technology of the laser beams, their use in practical systems has not yet been deployed.

Communication over deep-space distances is extremely difficult. Communications beams spread as the square of the distance between the transmitter and the receiver. As the distance increases, the difficulty becomes quadratically more difficult. For example, conventional satellite communication from Earth orbit often uses satellites in geosynchronous Earth orbit (GEO) to communicate with the ground. The GEO altitude is approximately 40,000 kilometers (km). From such a distance, quite high data rates in the gigabits per second (Gbps) can be established and maintained. However, the distance from Earth to Neptune or Pluto can be on the order of four billion (4,000,000,000) km. After propagating over such a distance, the communications beam from a spacecraft will spread to an area 10 billion times larger in area than if the beam from the same system traveled from just the GEO distance. The weakened beam would make communications with the Earth 10 billion times more difficult. Stated differently, a system capable of transmitting 10 Gbps from GEO to the ground would only achieve 1 bit per second (bps) from nominal Pluto/Neptune distances. One could, of course increase the capabilities of the distant spacecraft's communications system, as well as improve the sensitivities of the Earth reception systems. Indeed, both of these approaches are used for present-day deep-space missions. The net effect has been to raise the nominal data rates from Mars distances to the range of tens to hundreds of kilobits per second (kbps), with correspondingly lower data rates for the outer planets. But further increases are hard to accommodate. Current missions are already flying antennas that are difficult to squeeze into protective launch shrouds, and increases in transmitter power are discouraged due to the difficulties of both generating electrical power at far solar distances as well as removing the waste heat resulting from the corresponding inefficiencies of the various transmitter energy conversion components. On the Earth end, increasing sensitivity is likewise difficult. Current National Aeronautics and Space Administration (NASA) Deep Space Network (DSN) antennas are already enormous (34-m and 70-m diameters), and the receiving system low-noise amplifiers are already operating at but a few degrees above absolute zero. More advances in conventional communications capabilities are planned, and even larger improvements are being researched for future consideration, but practical realities will eventually limit the degree to which such improvements can be made.

As an example, consider the Mars Global Surveyor (MGS) mission that was, and continues to be, an outstanding success mapping features of the Martian terrain. During the entire prime mission phase, the project was only able to map 0.3 percent of the Martian surface at high resolution. More has been mapped during the extended mission phase, but even with this extension, the mission will produce high-resolution maps of only a few percent of the surface. This coverage has been limited by the capabilities of the communications system that was affordable at the time the mission was defined and developed.

Although conventional capabilities will likely rise in the future, so will the needs for even higher instrument data volumes. Most of the planets have had initial flyby pathfinder missions, and a few have had initial-characterization orbiters. However, the spatial and spectral sensitivities of those instruments have been very limited by the data-return capabilities and are orders-of magnitude below what scientists are doing for Earth observations today. Figure 1-1 shows these future needs. The horizontal axis is the data rate, and the vertical line near the left side is the MGS capability when scaled to Saturn distance. The vertical dimension has no meaning other than to show that things above the central data-rate-axis arrow are representative of scientific investigation needs, whereas those below just provide a rough measure of telecommunications needs for enhanced public engagement. The ovals represent horizontal data rate regions where corresponding instruments are expected to operate. Regions of anticipated capability improvements are shown for several candidate communications technologies. Technologies ultimately chosen and how far to the right those improvement bars can be extended depend on current and planned technical research and system designs, as well as thorough life-cycle-cost analyses. However, the anticipated performance capability improvements of optical communications are clearly evident.

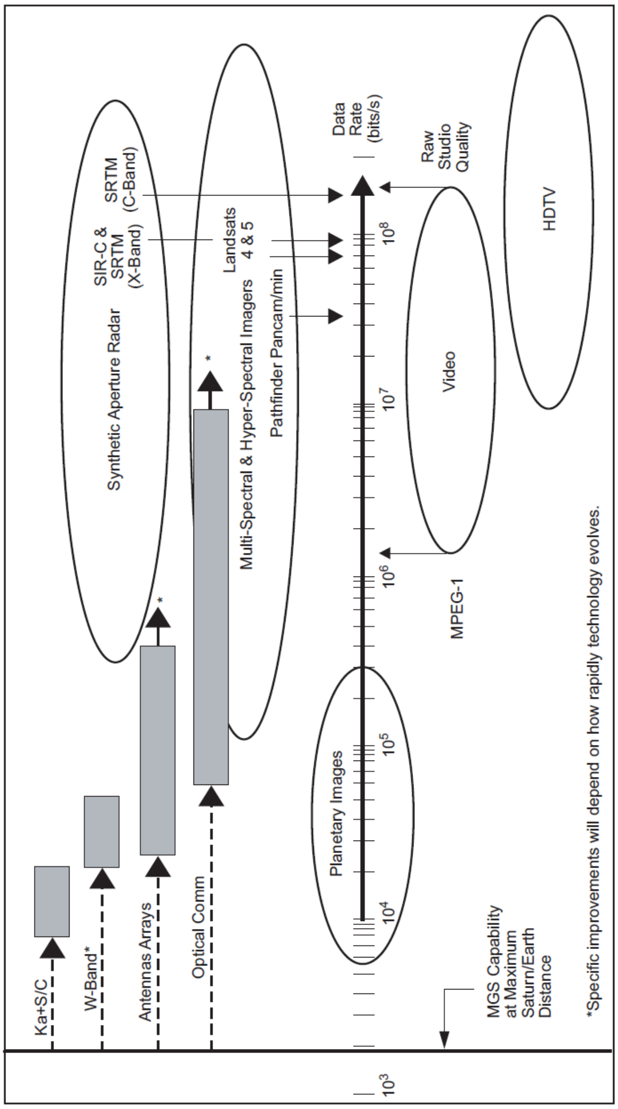

Fig. 1-1. Future data return needs relative to current capabilities based on Mars Global Surveyor at maximum Saturn range.

The promise of improvement comes, to first order, from the much higher frequencies of the optical signals. Over the history of the DSN, conventional RF performance has improved about 12 orders-of-magnitude due to significant and sustained research and development (R&D) efforts at JPL. Improvements have come from many technological advances. However, the biggest improvements were achieved when the operating carrier frequency of the communications signal was increased. Currently, the primary frequency used for deep-space communications is X-band (approximately 8 GHz), although new missions will soon be transitioning to Ka-band (32 GHz). The change from X-band to Ka-band has a theoretical improvement (due to frequency-squared) of 11.6 dB, although practical factors (e.g., atmospheric losses) have limited that improvement to about 6 dB. The promise of optical communications is much more since the frequency is very much higher (approximately 300,000 GHz). Although practical factors (e.g., atmospheric losses, receiver sensitivities) will also be present, they are more than offset by the frequencysquared benefit of the higher carrier frequency.

Figure 1-2 diagrams the much lesser beam spread offered by optical transmission. The left side of the figure shows the transmitted beam sent back toward the Earth from the Voyager spacecraft. The transmitting antenna is 3.7 m in diameter (a dominant architectural feature of the spacecraft), and the transmitted frequency is X-band. By the time the beam reaches Earth from Saturn, diffraction (a fundamental property of all transmitted electromagnetic beams) has caused the signal to spread out over an area 1000 Earth-diameters wide. Contrast this with the right-hand side of the figure where the beam from a small (10-cm) optical telescope is transmitted back to the Earth. Assuming an optical wavelength of 1 m (frequency of $3\ 10^{14}$ Hz), the resulting spot size at the Earth is only one Earth diameter wide. That represents a factor of 1000 concentration of the received energy in both the horizontal and vertical directions (factor of 10^{6} in power density), and that is achieved with a very much smaller transmitting antenna (0.1 m versus 3.7 m) on the spacecraft. The wavelength-squared advantage over X-band is approximately 90 dB, although quantum effects and practical implementation considerations limit current realistic gains to about 60 dB.

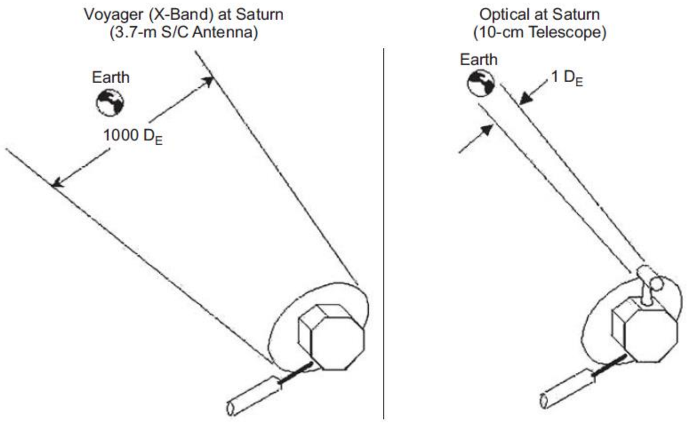

Fig. 1-2. Comparison of RF and optical beam spreads from Saturn.

An optical-communication system requires many component technologies. Virtually any one of them can be critical depending on the specific system requirements. It would be impractical to describe them all here, but there are a few component technologies that frequently make the critical list, and these are described below.

Laser Transmitters

One of the most important component technologies involves laser transmitters. When JPL began work in optical communications, laser transmitters had limited powers (less than 100 mW), their efficiencies were very low (less than 1 percent), and they were very unreliable. Some efforts, sponsored by the United States Air Force, had developed a cavity-dumped neodymium-doped, yttrium-aluminum-garnet (Nd:YAG) laser for possible space applications (later downgraded for an airborne laser communication demonstration), but its wall-plug power efficiency was about 0.5 percent). Such power conversion efficiencies were too low to be viable for deep-space missions where power generation is extremely difficult and costly. Building on research already underway at the California Institute of Technology (Caltech), JPL began doing research on monolithically integrated semiconductor laser arrays. Semiconductor lasers were much more power efficient than conventional solid-state (e.g., Nd:YAG) lasers, but their output powers were much lower. It was thought that by combining many laser diode elements together in a phase-locked array transmitter, the power output could be increased to the requisite (1–3 W average) levels, and the resulting transmitters would be extremely efficient (perhaps 40 percent). Additionally, one could also consider electronic beam steering of the beam from a laser diode array. Initial progress, both at JPL/Caltech and elsewhere, was very promising, and significant increases in power levels were achieved. Additionally, phase steering was demonstrated in many devices, but two problems remained. First, despite the increases in average power levels, the PPM modulation required that the laser energy be concentrated in high peak pulses. When the full average power levels of semiconductor laser arrays were concentrated into short-duration pulses, the instantaneous power densities at the laser facets far exceeded the device damage thresholds. Additionally, highpower laser arrays required efficient thermal conduction from the lasing epitaxial layer and hence required wafer-side mounting to the copper heat sinks. But, access to that same wafer side was required to control injection currents to accomplish electronic beam steering. Hence, the mounting required for highpower generation would short out all the control signal lines for the electronic beam steering.

The semiconductor laser arrays really functioned like efficient optical batteries (i.e., efficient converters of electrical energy to continuous wave (CW) optical energy). What was needed was the equivalent of an optical capacitor that could store and accumulate that optical energy until it was needed for a short optical (PPM) pulse. Nd:YAG laser rods could act as an optical capacitor, storing the optical energy in the fluorescent lifetime of the Nd ions, but they were just too inefficient in converting electrical energy into excited Nd ions.

In 1984, Don Sipes had an idea to improve this energy efficiency. He noted that the contemporary designs of Nd:YAG lasers surrounded the Nd doped YAG rod with laser diode pumps, but stimulated Nd:YAG laser emis ion along the central axis of the laser rod. Furthermore, the rod material was highly absorbent at the pump laser wavelength (by design), giving rise to very high excitation levels near the circumference of the rod, but the pump power density in the region of the rod where lasing occurred was much lower. He then reasoned that if he could inject the diode laser pump energy along the same axial space where the laser cavity mirrors were stimulating the Nd:YAG laser emission, then the conversion factor would be much better. This could be done with proper anti-reflection coatings on the cavity mirrors. Additionally, if both the pumping mode and the lasing modes were made very small in diameter inside the rod, then the conversion factor would be even larger. With a research investment of only a few thousand dollars, he assembled such a laser that produced greater than 5 percent electrical conversion efficiency on the first try.

Further improvements on this approach over the years have increased the power levels to more than 10 W. Aa later version of this design that produced 2 W of pulsed and frequency-doubled (green, 532-nm) output laser power, and up to 11 W of pulsed laser power at the Nd:YAG fundamental wavelength of 1064 nm. This design demonstrated that laser powers and efficiencies realistic for deep-space optical communication were possible. This laser structure was the only viable deep-space laser approach for almost 15 years until fiber-amplified lasers began to emerge.

Spacecraft Telescopes

Another key technology component is a thermally stable and lightweight optical spacecraft telescope. Serving as the optical version of an antenna, this telescope was required to keep surface deformations under a small fraction of an optical wavelength (a small fraction of a micrometer [�m]) and to do so over a large temperature range.

Thermally stable glasses had been used in many applications, but they required too much mass. Through a Small Business Innovative Research (SBIR) contract with SSG Inc., a 30-cm-diameter telescope that was very precise and thermally stable was developed. Made entirely of silicon carbide, the telescope had a mass of only 6 kg.

Acquisition, Tracking, and Pointing

As mentioned above, one of the most important reasons for considering optical communications is the narrow beam divergence that allows the transmitted power to be concentrated on the receiving target location. However, that narrow divergence benefit comes with the penalty that the beam must be precisely pointed, or the entire benefit is lost. This pointing must be accomplished in the presence of attitude changes of the host spacecraft that are perhaps a thousand times larger than the laser beam divergence. Additionally, platform jitter disturbances can be many beam-widths in magnitude and can have characteristic frequencies of a hundred or more hertz. Finally, the transmitted beam from a spacecraft must be offset (pointed ahead) from the apparent location of the receiving target to compensate for cross velocities between the host spacecraft and the reception location. The normal way of accomplishing all these functions is for the spacecraft terminal to acquire and track an uplink beacon signal from the intended receiving target. That beacon is used to precisely calibrate the attitude orientation of the spacecraft's transmitting aperture. The beacon signal is also used to measure the vibrational components of the host spacecraft. Correction of both the telescope line-of sight error, as well as compensation for vibrational disturbances, is then accomplished using one or more fine-steering mirrors in the optical path to the telescope. This compensation scheme can also be used to implement the needed point-ahead angle calculated from mission trajectory and planetary orbital predictions. Initial work at JPL in the late 1980s resulted in the development of an Integrated Optical Communications Test Bed (IOCTB). The IOCTB contained the necessary components to simulate a beacon signal and accomplish the required beam-pointing functions. It served as a familiarization test bed until newer acquisition, tracking, and pointing techniques were developed. One of the early concerns was the difficulty of getting a sufficiently strong laser beacon signal out to a spacecraft when it is at one of the outer planets. As an alternate approach, techniques were investigated that relied on the solarilluminated Earth itself as a beacon. Several strategies have been investigated over the years that use different tracking reference sources, either rom visible sunlight reflected off the Earth or from the infrared emissions of the Earth as seen against the cold sky background. To date, while promising, these techniques have yet to prove that they can provide adequate reference signals under all the various conditions and still be competitive with direct beacon tracking. JPL has also investigated, as a hybrid technique, tracking of a weak uplink laser beacon signal used in conjunction with inertial sensors (e.g., accelerometers) to measure the vibrational components of the spacecraft. This approach is much more promising and allows the weak uplink beacon to be integrated longer to determine the spacecraft absolute attitude, while the inertial sensors permit compensation for the higher-frequency vibrational components

Detectors

Another crucial component technology is that of detectors. Both detectors for optical-communication data extraction and detector arrays for spatial acquisition and tracking are needed. For data channel detection, the detector used in the multi-bit/photon demonstration was an RCA 31034C PMT. However, this and similar PMTs suffered from two problems. First, their quantum efficiencies at the primary candidate operational wavelengths were too low (typically less than 1 percent). Second, the tubes had such high gains that nominal background and/or strong signal levels would likely cause output currents that exceeded the anode plate current limitations. Clearly some other kind of detector was needed. An alternative is to use an avalanche photodiode detector (APD). Normally, APDs are operated in a mode where a bias voltage up to, but not exceeding, the spontaneous avalanche breakdown voltage is applied. The higher the voltage, the higher the gain, but also the higher the rate of spontaneous dark-count-generated detection events. Furthermore, the output resulting from the avalanche gain of the detected signal had a high variance, resulting from random multiplication gains through the photodiode's lattice structure. Although often higher in quantum efficiency, such detectors were not suited for detection of single photons.

In 1985, JPL began looking at APDs that were biased beyond the avalanche breakdown voltage. In this case, the gains would be high enough to detect single photon arrival events. Under normal conditions this would result in a constant avalanche condition due to thermally generated carriers in the photodiode. However, by cooling the APD nominally down to about liquid nitrogen temperatures, the thermal carrier generation process could be significantly suppressed. That would leave the photodiode detector ready to trigger a massive avalanche, but with most of the thermally generated false detections eliminated. The result would be an optical detector that operated similarly to the way a Geiger counter works on radioactive detection events. To verify this, a test setup was created, and APD detectors were tested under single-photon input level conditions. Greater than 30 percent quantum efficient detection of single photons was demonstrated.

One of the problems identified in these "Geiger-mode" detectors was that after a triggered event occurred, whether from an incident signal or background photon, or from a residual thermally generated carrier, the avalanche process would have to be stopped (or quenched). One way to quench these avalanches was to place a resistor in series with the APD. When an avalanche would start, the voltage drop across the resistor would reduce the voltage across the APD to below the avalanche breakdown voltage, thus stopping the avalanche. However, the resistance of the load resistor, coupled with the junction capacitance of the APD, resulted in a relatively large resistance–capacitance (R–C) time constant, thus overly limiting the bandwidth of the detection system. An alternate approach was to build an active quenching circuit that would rapidly trigger an electronic voltage interrupt. Unfortunately, such circuits were difficult to design and operate at that time.

More recently, work has been done on operating commercially available APDs at voltages just under the avalanche breakdown voltage. Since the voltage is high, the gain, and hence detectivity, is also high. But, since the detector is operated below avalanche breakdown, the detector does not lock up in a sustained avalanche, and the output resembles an amplified version of the input. Additionally, by cooling the detector, the resulting dark count rates can be minimized. Single-photon detection efficiencies greater than 30 percent have been demonstrated

The other major detector needed is a detector array for the spatial acquisition and tracking system on the spacecraft. This detector is used to track the location of a beacon signal from the intended receiving location and often a portion of the outgoing transmit beam signal for precision beam pointing. The detector must have a large-enough field of view to cover the attitude uncertainty of the host spacecraft (often several milliradians [mrad]), yet produce final spatial resolution measurements that are a small fraction of a transmitted beamwidth (resolutions well below a □rad). Furthermore, the detector must be read out fast enough to compensate for higher-frequency vibrations on the spacecraft that would cause excessive beam jitter. Conventional charge-coupled device (CCD) detector arrays have adequate field of view (FOV) and resolution, but the typical frame rates (10–30 Hz) are inadequate to follow higher-frequency jitter components. A significant amount of effort was then directed toward windowed CCD arrays. With a windowed array, only small regions (typically 10 10) around the desired spatial tracking points need to be read out; after which, the rest of the array signal can be dumped and the next image taken. By windowing, the repeat time to the desired tracking points (after acquisition has occurred) can be fast enough to track even the higher-frequency jitter components. In the future, even more efficient tracking detectors will be possible with the use of active pixel sensor (APS) detector arrays. With APS detectors, the signals from the windowed regions of interest will not need to be read off the detector chip. Instead, it will be possible to process the signals into real tracking information via on-chip complementary metal oxide semiconductor (CMOS) processing.

Filters

On the receiving end of the link, narrow-band filters will be required before the detectors, especially if daytime reception on the ground is to be used. Narrow transmission bandwidths will eliminate much of the background light interference, but the throughput efficiencies must be high to avoid causing significant loss to the desired signal. Multi-dielectric filters are the commonly used filters, but they are limited in how spectrally selective they can be and still have adequate throughput. One filter investigated in this category is the Fraunhofer filter. In the solar spectrum, there are narrow regions where the solar energy is trapped by certain elements in the Sun's photosphere. These are regions of the solar spectrum where the Sun is effectively dark (or at least not so bright). By selecting a laser line that corresponds to a Fraunhofer line, and then using an interference filter matched to that line, communications can take place with significantly lower background interference levels. One of the laser wavelengths of early interest was that of a frequency-doubled Nd:YAG laser at 532 nm. Several spectral dips exist in the solar spectrum near 532 nm. To achieve really narrow passbands (less than 1 nm) it is necessary to use filters that are based on atomic transitions in materials. Atomic resonance filters (ARFs) can produce sub-nanometer bandwidths. However, these filters cannot be used in front of acquisition and tracking systems since the filtering operation relies on the absorption of a photon at one wavelength and the corresponding emission of another at a new wavelength. The creation of the new photon is dependent on the energy absorption of the input photon, but its angular direction is not preserved. To get around this, work was done in the early 1990s on the development of filters that produced polarization rotations as a result of the anomalous dispersion shifts of certain pumped gasses. Two versions were studied: the Faraday anomalous dispersion optical filter (FADOF) and the Stark-shifter anomalous dispersion optical filter (SADOF). Both filters work by passing polarized light into an atomic cell. If the input light is precisely on resonance with the excited gas in the cell, the input light will undergo a polarization rotation due to the anomalous dispersion of the gas. Light that is not precisely on resonance (i.e., background light) will pass though the cell but without the polarization rotation. By placing a crossed polarizer at the output of the cell, only the on-resonance light is allowed to pass. Furthermore, since the light is not absorbed and then re-emitted, the angular direction of the on-resonance light is preserved.

Error Correction Coding

The last, but by no means the least, component technology to be discussed is optical coding. As mentioned earlier, the original multi-bit/detected-photon demonstration used high-order PPM modulation (256-PPM) with a high alphabet (8-bit alphabet) RS code. The RS alphabet was matched to the PPM modulation since each 8-bit character would specify which of the 256 pulse locations would be used for that character. The prevailing belief was that the higher the order of the PPM modulation, the better the performance, provided the modulation was used with a matching-alphabet RS code. However, as the PPM order increased, the matching RS alphabet (and hence code) became much more complex. Furthermore, it was known that if the PPM order was reduced (along with its matching RS code), performance of the link was significantly reduced. This usually forced system designers to consider only high-order PPM modulations, but high-order PPM meant a high value of peak-to-average power level from the laser since the laser's average power was concentrated in a much narrower (and infrequently filled) pulse slot. Laser power limitations became a constraint on how high the order of the modulation could be. Recent progress has been made in the development of codes that can relax the need for higher-PPM formats, and hence the required peak-to-average power levels of the lasers [66–70]. The codes (called accumulator codes) are based on product-coding techniques where simpler codes are combined and then jointly (and iteratively) decoded. One of the benefits is that one can start with a lower-PPM alphabet that is further from the overall channel capacity limit and regain a large portion of the lost performance with coding. Going to higher-order PPM modulations and using a good code over that modulation is still better in terms of performance, but the difference between properly coded lower-order modulations and properly coded higher-order modulations has diminished. Table 1-1 gives a comparison of several different PPM modulation orders and corresponding coding gains from the accumulator codes. Note the higher coding gains for the lower PPM orders.

Table 1-1. Coding gains of accumulator codes (in dB) for various PPM modulations.

PPM Order	2048	256	16	4
Gain relative to RS code	2.25	2.78	4.82	9.08
SNR gap to capacity (dB)	1.26	1.29	1.03	1.08
Optimal constraint length	2	2	3	4
Average iterations required	9	9	7	6

Optical Transceiver Package (OPTRANSPAC)

The first flight terminal system design was the Optical Transceiver Package (OPTRANSPAC) study conducted it 1984. It was a contracted study with McDonnell Douglas Corporation and leveraged their prior work for the United States Air Force on the Airborne Flight Test System and subsequent development activities for the Defense Support Program's (DSP's) planned Laser Crosslink System (LCS). The design had independent detectors for spatial acquisition, spatial tracking, and uplink data detection. The design was being performed as a pre-project study for a possible flight demonstration on the Cassini deep-space mission to Saturn. The OPTRANSPAC system design had a 28-cm telescope, had a 400-mW (frequency-doubled Nd:YAG) laser, and would return a 100-kbps communication flow from Saturn to a 10-m-diameter Earth-orbiting receiving aperture. The mass and power consumption estimates were 52 kg and 57 W, respectively, and the terminal occupied a volume of approximately 0.1 m3. At the time, the mass was considered too much for the Cassini mission to fly as a mission-enhancement demonstration, so the fullscale development was not continued. However, the OPTRANSPAC study results were used as a basis for the IOCTB development mentioned earlier. A sketch of the OPTRANSPAC terminal design is shown.

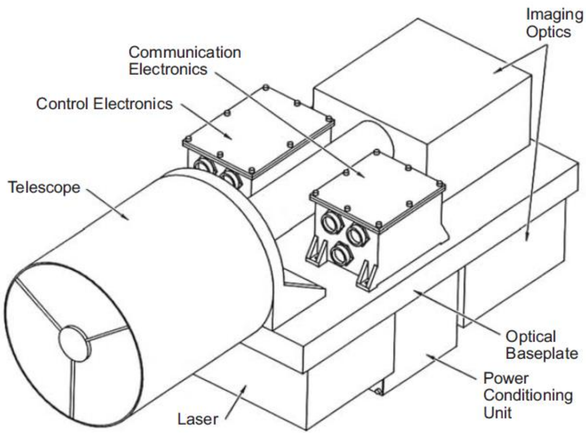

Optical Communications Demonstrator (OCD)

One of the attributes of the OPTRANSPAC design was that it used separate detectors for acquisition, for tracking, and for beam point-ahead (the offset angle needed to lead the Earth-station receiver when there is relative crossvelocity between the two ends of the link). Additionally, there were separate fine-steering mirrors to implement the necessary beam centering and offset functions. Detectors and steering mirrors are primary optical system components, but they usually need secondary elements (e.g., focusing lenses and beam-folding mirrors) to make them work properly. All these components must be precisely held on thermally stable structures in space terminals. This meant that if the basic design of a flight terminal had a lot of primary components, then the overall complexity, mass, and cost of the terminal would be much higher due to all the elements (primary components, secondary components, and supporting infrastructure) required to make the end system function properly. By realizing this relationship, it was conversely realized that if the number of primary components could be reduced, then the number of secondary components would also be decreased, as would the requirements for the supporting structure. This realization led to the basic design of the Optical Communications Demonstrator (OCD). The fundamental design for the OCD is shown. The OCD concept works as follows. A beacon signal is sent to the flight terminal from the intended receiving terminal. That signal is received on the flight terminal by its telescope (depicted by just a lens in the diagram for simplicity). The telescopecollects the beacon signal and focuses it to a point on the receiver focal-plane array in the terminal. The location of this spot on the array represents the direction from the received beacon signal relative to the telescope's axis (the center of the array). The array size determines the field of view of the telescope and is large enough to cover the initial pointing uncertainties of the telescope (often defined by the attitude control dead-band limit cycle of the spacecraft). No overt effort is made to center the received beacon signal on the focal-plane array. This just represents the knowledge of the direction to the receiver. The modulated laser signal that is to be returned by the flight terminal to the ground receiver is coupled (via optical fiber) into the OCD assembly and initially strikes a two-axis steering mirror. After reflecting off the steering mirror, it passes up to a dichroic beam splitter that reflects almost all the signal out of the telescope. However, there is a small amount of signal that passes through the dichroic beam-splitter and progresses upward to a retro-reflector. The retro reflected signal returns to the backside of the beam-splitter where it is directed toward and focused onto the focal-plane array. This spot location represents the direction of the outgoing laser signal relative also to the telescope axis. The vector difference between the focused beacon signal and the focused residual of the laser transmit signal on the focal plane represents the angular difference between the received and transmitted directions and is independent of the axis of the telescope. (The actual axis of the telescope is common and drops out in the vector difference.) Now, as stated earlier, there is a need to implement a point-ahead angle to the transmitted beam. This can be done by simply monitoring the vector difference between the two focused spots and making sure that it represents the needed point-ahead angle (which can be easily calculated given the orbital predicts and the nominal spacecraft-orientation information.

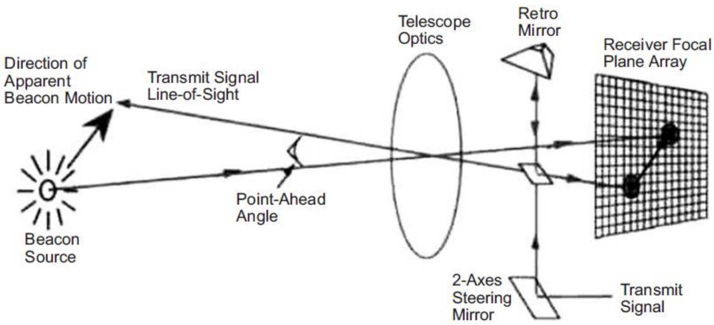

X2000 Flight Terminal

The next major flight terminal design effort was undertaken as part of the X2000 program. The X2000 program was initiated to fill the gap of major needed technology developments required for future missions. It was recognized that because of the NASA shift to faster-better-cheaper (FBC) missions, the technology developments that had customarily been developed as part of the former "flagship" missions would no longer be possible.

Development of an optical communications flight-qualified engineering model terminal for a proposed Europa Orbiter mission was the second largest planned development in the program. First, the diameter of the telescope was increased to 30 cm. This was based on the successful development of the silicon carbide telescope mentioned earlier. Second, it was realized that the basic structure of the OCD contained a telescope and a focal plane array, the two primary components in an imaging camera. Third, an uplink command detector path was added. Since this detector was a high-speed detector, it could also serve as an uplink ranging detector for an optical turn around ranging system. Thus, the requirements for the X2000 design included dual-use as a science imaging camera and as an uplink reception capability for command and ranging. Furthermore, the proposed Europa Orbiter mission study team was considering the use of a laser altimeter. It was realized that the optical communication telescope and high-speed uplink detector could also be used as the laser altimeter return signal receiver/detector.

The X2000 optical communications development proceeded to the point of a concept design. However, budget pressures in the rest of the X2000 program ultimately caused cancellation of all X2000 developments except for the primary element, a spacecraft computer/avionics system. The optical communications terminal design had been progressing well, but the application time frame for the technology was considered to be far enough to accommodate the delayed development.

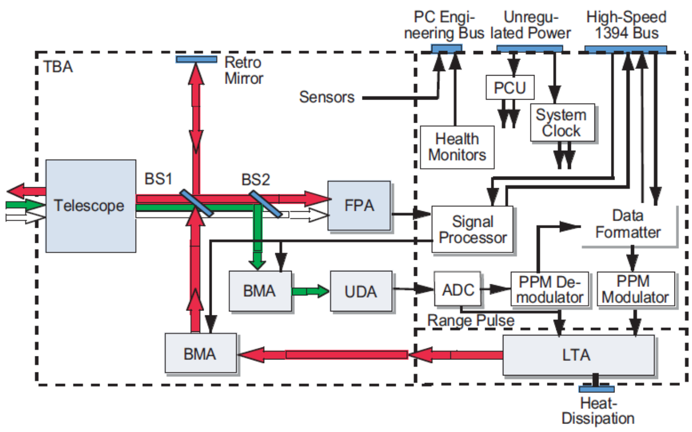

ADC = Analog-to-Digital Converter
BMA = Bi-Axis Mirror Assembly
FPA = Focal Plane Array
LTA = Laser Transmitter Assembly
PCU = Power Conditioning Unit
PPM = Pulse Position Modulation
TBA = Telescope & Beam-Optics Assembly
UDA = Uplink Detector Assembly

International Space Station Flight Terminal

Another flight development program came along a few years later. In 1996, a NASA call was released for payloads that could be demonstrated on the International Space Station (ISS). The objective was to use the ISS as an engineering center for such demonstrations. A proposal was written, and in 1997 the proposal was selected for development. The program was funded under the ISS Engineering Research and Technology (ISSERT) program that also funded a number of other attached payload developments. The terminal design was based on the OCD architecture, and the plan was to transmit at least 2.5 Gbps from a terminal mounted on the ISS external nadir-pointing truss to the ground. The flight terminal would be developed and integrated with the ISS express pallet, for subsequent transport in the Space Transportation System (STS or Space Shuttle) to the ISS. The ground terminal would be a new Optical Communications Telescope Laboratory (OCTL) that was already funded under the Deep Space Mission System (DSMS) Technology Program. The operational concept included an uplink beacon from OCTL to the ISS mounted terminal. The flight terminal would spatially lock onto that beacon and transmit down a pseudo-random coded data stream. Early in the program development, the ISSERT management at NASA Johnson Space Center realized that the optical communication terminal represented a valuable resource that would likely be underutilized. As a result, they initiated a change order to provide an optical-fiber transfer line from the interior of the ISS to the optical communication terminal location on the external truss. This would allow real data to be sent over the optical link to the ground. Unfortunately, as was the case in the X2000 development, budget pressures were heavy here as well. The program progressed through Phase A and had just completed its preliminary design review (PDR) when budget pressures related to the building of the core ISS resulted in cancellation of all attached payload developments, including the optical communication terminal.

Ground Telescope Cost Model

The first serious look at the definition of a ground receiving system was done in 1986 and involved establishing a cost-versus-performance model for ground-based telescopes. The study started with a set of data on existing RF, solar concentrator, and optical astronomical telescopes. When the costs of those telescopes were plotted as a function of diameter, it was noticed
that the costs could be modeled as

C = Dx

where C was the cost (in $M), D was the diameter of the telescope (in meters), and x was a value that varied between 2.4 and 2.8 (taking 2.6 as a nominal value). The value of was dependent on the inverse of the telescope's focused blur circle diameter "F" and was approximately given by

=105 / F

Next, the performance of communication link was calculated as a function of telescope diameter and blur circle using a reference transmitter and a set of background conditions. Since the cost and the performance could each be calculated based on the same two parameters (diameter and blur circle), then the cost of the telescope could beplotted as a function of communication performance with telescope diameter and blur circle diameter as parameters. Upon optimizing over diameter and blur circle, one then had a plot of optimized-cost-versus-communications
performance.

Next figure shows the results of this analysis but extrapolated to a worldwide network. The analysis showed that the knee of the cost curve occurred at about 18 dB of improvement over the reference X-band link. The values of the optimized parameters in this region were a 10-m-diameter telescope and a blur circle that was larger (less precise) than the diffractionlimited focus. This result was intuitively satisfying since it was known that 10-m-diameter diffraction-limited telescopes could be quite expensive but that similar-sized solar concentrators were much less expensive. Since nondiffraction- limited telescopes were essentially photon buckets, then this also meant that direct detection of the received signals could be used, and there would not be a need to compensate for atmospheric turbulence-induced phase fluctuations.

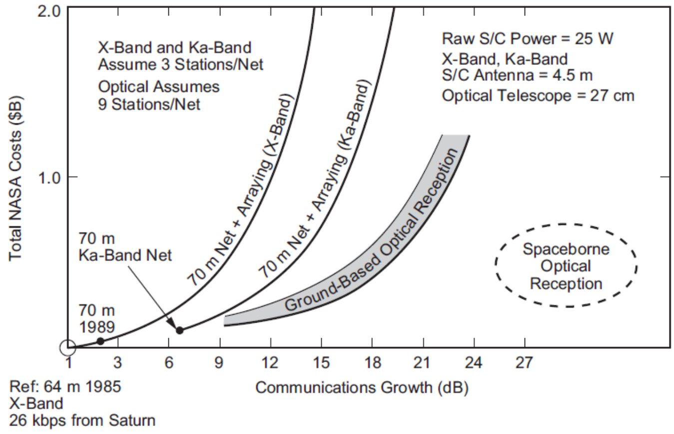

Deep Space Optical Reception Antenna (DSORA)

Given the insight afforded by the cost-modeling effort, a series of studies was conducted to define, analyze, and estimate the cost factors for various realizations of a 10-m-diameter photon bucket. These generally went under the name of Deep Space Optical Reception Antenna (DSORA). Early in the process, it was realized that some form of sunshade would be important if the system was to be used in the daytime, especially if that use was directedanywhere close to the Sun. Several sunshield concepts were explored, including the use of an external tube outside, but connected to, the dome. The favored approach was an "integral" sunshield that followed the "soda straw bundle" concept. The idea was to collect together a set of hexagonal tubes that had cross-sections the same sizes and shapes of the primary mirror segments. These would be placed over the primary collector surface, but with the lower portions of the central "tubes" shortened so that the ray paths from the primary mirror segments would not be blocked from getting to the secondary mirror. Since the length/diameter (L/D) ratio of each "tube" was large, the telescope/sunshield could point much more closely to the Sun without direct sunlight hitting the primary mirror surface. The remaining challenge, however, was the fact that the tubes became good collectors of solar radiation (heating), and there was concern that unacceptably large turbulence would result. Several concepts, including the use of "expanded metal" (similar to that used in window screens), were considered to mitigate
this effect.

Ground-Based Antenna Technology Study (GBATS)

In parallel with the DSRSS studies, JPL performed an updated study on ground-based optical receivers. The study, dubbed Ground-Based Antenna Technology Study (GBATS), considered both the details of the design for a 10-m optical reception ground station as well as the overall operational network architecture using such stations as element nodes. The design of the 10-m telescope consisted of a segmented primary aperture with active control of the primary segments (to control low-bandwidth aperture distortions caused by gravity loading, thermal distortions, and wind buffeting). Furthermore, a collapsible dome structure similar to an existing United States Air Force 3.5-m telescope was included. For the network architecture, it was necessary to consider spatial-diversity reception from the beginning to circumvent cloudcover outages. Two fundamental architectures were considered. The first consisted of three clusters of three optical telescopes in each of the three current DSN RF antenna regions. This would allow the three-longitude paradigm of the current DSN to continue. However, for spatial diversity benefits, each of the clusters at each longitude would have to be spread out over several hundred kilometers to be in different weather cell regions. This automatically implied a network of nine stations. For the other architecture, the constraint that the stations needed to be somehow “clustered” around an existing DSN station longitude was removed. This allowed the stations to be located in a pattern where one could act as a redundant neighbor for any of the stations in its neighboring longitudes. Networks of 6, 7, and 8 stations dispersed linearly in longitude around the globe were considered. It was found that the linearly dispersed optical subnet (LDOS) approach, rather than the DSN-centric “clustered” approach, was the more cost effective.

Atmospheric Transmission

In order to design a deep-space-to-ground optical communications link, it is necessary to understand the losses that will occur as the signal propagates through the atmosphere. Both cloud blockages and atmospheric molecular absorption will impede the signal. Understanding the statistics on these losses is crucial so that the requirements for diversified reception (i.e., number of stations) and the resulting communications reliability can be determined. Molecular absorption is based on the percentages of different molecules in the atmosphere, and this effect can be reasonably well predicted using software tools developed over many years by the United States Air Force Research Laboratory (AFRL). As long as the wavelength used for communications does not lie on or very near a strong atmospheric absorption line, the clear-weather link attenuation is relatively constant. Clouds, on the other hand, occur much more randomly and can result in total extinction of the optical signal. To assess cloud-cover statistics, JPL first obtained cloud-cover statistics taken from the Geostationary Operational Environmental Satellite (GOES) system. These statistics were in the form of cloud-cover contour maps provided by the University of Wisconsin, and clearly showed that clear skies are much more likely in the southwestern U.S. However, when comparing statistics, it was also evident that the sum of the clear-sky and cloudy-sky probabilities for a given spot was less than 1. The remaining probability mass is a result of partial cloudy conditions. Furthermore, it is important to know what defines clear or cloudy. Thin cirrus clouds may not show up on a satellite images as clouds, but they still result in some, albeit not always large, attenuation of the signal. Realizing the need for more detailed statistics on atmospheric throughput, JPL created a program to make in situ measurements of the atmospheric throughput attenuation. To accomplish this, three atmospheric visibility monitoring (AVM) observatories were built and deployed in the southwestern U.S. One is located at Table Mountain, California, a JPL astronomical observatory site near the town of Wrightwood. The second AVM observatory is located at the DSN’s Goldstone Deep Space Communications Complex north of Barstow, California. The third is located on Mount Lemmon in Arizona. Each AVM observatory contains a 25-cm telescope, a detector array, and several spectral filters on a filter wheel. The system is housed in a roll-off roof enclosure that is connected to a weather-sensing suite. The system operates autonomously, both day and night, to gather atmospheric throughput data by monitoring stars and measuring the stellar intensity on the ground in six spectral bands. By comparing the measured intensities of stars with the abovethe- atmosphere values for those stars, the atmospheric throughput can be measured. The weather-sensing tower monitors for conditions at the site that would make telescope observation unsafe (i.e., high winds, rain/snow, excess humidity), and if such conditions are sensed, the enclosure roof and fold-down south-facing wall will close. Any time the enclosure is closed, or the system is not able to detect a star, the resident computer declares that the sky was totally cloudy. Otherwise, the observatory makes measurements of the stellar intensities and records them on the computer. Data are routinely transmitted back to JPL for processing and statistics generation.

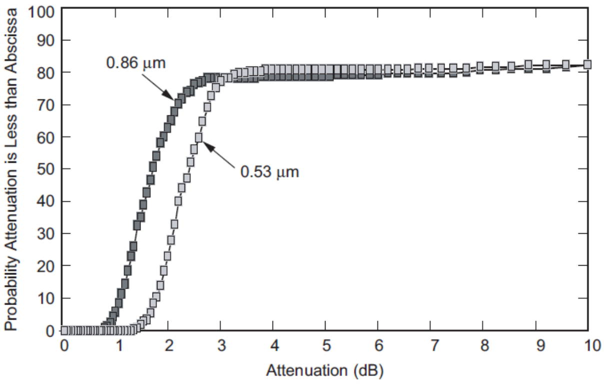

The Future

This past experience base provides a springboard for many of the planned activities of the future. These are both developmental activities as well as some exciting system demonstrations. Many of these will use the infrastructure already created, whereas others will result in the development and validation of new systems, tools, and techniques.

Optical Communications Telescope Laboratory (OCTL)

One of the key infrastructure elements recently created is the Optical Communications Telescope Laboratory (OCTL). Located at JPL’s TMF, OCTL will be the main ground support facility for a number of planned free-space optical communications demonstrations. Although there are a number of telescopes already at TMF, they are not well suited for use in the emerging set of planned demonstrations. Most of the current telescopes have inadequate space in their focal planes to accommodate the optical and electronic systems needed for planned future demonstrations, and none of the telescopes was designed for use during the daytime. The OCTL telescope is a 1-m-diameter diffraction-limited telescope that has a coudé focus and four coudé instrument rooms. Separate demonstrations can be set up in each of the coudé rooms. The telescope axis can be connected to one of these rooms by a coudé-room fold mirror (designated as M7). This will allow the telescope to be used while other demonstration setups are being installed in other rooms. Furthermore, the telescope is designed to operate within its diffraction-limited wavefront error tolerances down to solar offset angles of 30 percent. Although its wavefront errors will be degraded at smaller solar angles, the thermal control system will allow it to function at even smaller solar angles. Additionally, the telescope mount is capable of precision tracking of low-altitude satellites. This will allow it to support demonstrations that are relevant to near-Earth applications as well as deep-space applications.

Unmanned Arial Vehicle (UAV)–Ground Demonstration

One of the planned early demonstrations involves optical communications from an uncrewed airborne vehicle and the ground. Funded by the United States Missile Defense Agency, this activity will fly a modified version of the OCD terminal called the Optical Communications Terminal (OCT) on a Predator B unmanned aerial vehicle (UAV). The OCT will be outfitted with a 1550-nm laser transmitter and will transmit at 2.5 Gbps from the UAV to the OCTL telescope. Reference [160] describes the UAV–Ground Demonstration program.

Adaptive Optics

One of the key technologies to be validated in the OCTL will be AO. As mentioned above, turbulence in the atmosphere can cause significant beam wander and intensity fluctuations on uplink beacon or command signals sent to distant spacecraft. Additionally, turbulence causes broadening of focused signal energy at the focal planes of ground-based receive telescopes. This broadening can drive the requirements for the detectors and result in increased susceptibility to background light interference. Under internal funding, JPL has been examining the use of AO techniques for optical communications. AO techniques have been used in the past and are becoming commonplace on many astronomical observatories. Indeed, the JPL work is building directly on experiences gained by implementing AO on the Palomar and Keck telescopes. These techniques have been used to sharpen images and enable astronomers to distinguish closely spaced celestial objects. However, unlike astronomy observatories, optical communication ground stations must also operate in the daytime. This exacerbates the levels of turbulence that must be accommodated. Additionally, the overall objective is different for optical communications relative to astronomical observations. For astronomy, the objective is to increase the sharpness of images so that the finest details can be observed. If in the process there is a loss of signal energy, then that loss can be made up by just observing longer. For communications, the signal energy devoted to a given data bit is fixed, and must be conserved as much as possible. Thus, the optimization function for an optical communication AO system is to minimize the overall field of view (to minimize the amount of background light admitted) while maximizing the amount of desired signal energy captured (for the most robust signal detection). For uplink beacon and command links, the multi-beam transmission technique mentioned in the GOLD demonstration can be used to reduce some of the beam intensity fluctuations. Increased transmit power is easier to generate on the ground so that the beams can reach further into space. But, to reach even farther, or to reduce the uplink power requirements for a given distance, uplink AO will be beneficial. Such systems will likely rely on artificially generated laser guide-star calibrators to accomplish the uplink signal adaptation. Both downlink signal-to-noise-ratio improvement and uplink beam-adaptive pre-distortion techniques can be validated using OCTL.

Alternate Ground-Reception Systems

Work is also under way to assess alternate architectures for ground-based reception telescopes. In 2001 a JPL internally funded study was started to examine the use of a collection of smaller telescopes to act effectively as a single large telescope. Initial results indicate that, for ground-based reception systems, arrays of small telescopes, each with its own focal-plane detector system, can be an attractive alternative to large single-aperture-reception telescopes, especially if each telescope includes a focal-plane detector array for electronically tracking the atmospheric turbulence-induced "hot spots". Given these preliminary findings, an experimental program was initiated to validate the projections of such an array. A JMI Inc. 63-cm-diameter New Technology Telescope (NTT) was procured, and initial tests have begun. Although the results are promising, the ultimate conclusions will depend on a thorough understanding of the performance characteristics of both large single aperture and arrayed smaller-aperture telescope architectures, as well as complete life-cycle-cost analyses of both approaches.

Current and Upcoming Projects in the United States, Europe, and Japan

The concept of free-space optical communications was conceived shortly after the invention of lasers. Strides have been made in developing and demonstrating the technology ever since. Early experiments that targeted terrestrial point-to-point, air-to-ground, and space-to-ground links were not fully successful because the technology was immature. Most of these demonstrations were government-funded, both for civilian and military applications. The promise of laser communication, high data-rate delivery with significantly reduced aperture size for the flight terminal, led to the continued funding for the successful experiments and provided the incentive for further demonstrations. The following Table presents a chronological summary of major successful laser-communication technology demonstrations to or from air or space. Plans for additional major experiments are discussed below.

Year	Experiment	Performing Organizations*
1980	AFTS (Airborne Flight Test System) 1 gigabit per second (Gbps) link from aircraft [1]	McDonnell Douglas (U.S. DoD)
1990	RME (Relay Mirror Experiment) Precision laser beam pointing [2]	Ball Aerospace (U.S. DoD)
1992	GOPEX (Galileo Optical Experiment) Uplink from Earth to deep-space [3]	JPL (NASA)
1995	LCE (Laser Communication Experiment) Bi-directional link from terminal at geosynchronous Earth orbit (GEO) [4]	CRL (Japan) and JPL (NASA)
1998	GEOLite (Geosynchronous Lightweight Technology Experiment) Multi-Gbps link from GEO orbit [5]	Lincoln Laboratory (U.S. DoD)
1998	SILEX (Semiconductor Intersatellite Link Experiment) Low Earth orbit (LEO) to GEO and LEO- and GEO-to-ground [6]	ESA

* Organizations Listed: Communication Research Laboratory (CRL), U.S. Department of Defense (DoD), European Space Agency (ESA), Jet Propulsion Laboratory (JPL), National Aeronautics and Space Administration (NASA)

LUCE (Laser Utilizing Communications Experiment)

The Optical Inter-orbit Communications Engineering Test Satellite (OICETS) carrying the LUCE payload is planned for launch into low Earth orbit (LEO) in 2005. LUCE has an aperture diameter of 26 cm and is equipped with 200-mW 847-nm diode lasers for 50 megabits per second (Mbps) transmission to the European Space Agency's (ESA's) Advanced Relay and Technology Mission Satellite (ARTEMIS). It is capable of receiving 2.048-Mbps links from ARTEMIS at 819 nanometers (nm).

Mars Laser-Communication Demonstrator (MLCD)

NASA is planning for the first deep-space laser-communication downlink in the 2009–2011 time frame from Mars distances utilizing the Mars Laser Terminal (MLT) being built by the Massachusetts Institute of Technology (MIT) Lincoln Laboratory flying aboard the Mars Telecom Orbiter spacecraft. MLCD will demonstrate data rates on the order of 1 to 80 Mbps from the longest distance (about 2.4 astronomical units [AU]) to the shortest distance (about 0.67 AU), assuming a 5-equivalent-diameter aperture. This data rate is at least an order of magnitude higher than state-of-the-art RF Mars communication systems.

2. Optical Wireless Communications (OWC)

2.1. Wavelength

Ever since the discovery of lasers in the early 1960, OCW has been as an alternative solution to support high speed data instead of radio frequency (RF) systems [2]. In every optical system, the first critical question is the operating wavelength. For space-based optical applications, the operating wavelength depends upon the trade-off between receiver sensitivity and pointing bias due to thermal variations across the Earth's surface. Generally, longer wavelengths are preferred as they cause reduction in solar background and solar scattering from the surface of the Earth. **Wavelengths currently being considered for space communication are in the range 0.5 µm to 2 µm.**

Over three decades of efforts towards intersatellite laser links, started by the 1980s European SILEX demonstration, have seen various technologies starting from those based on lamp pumped mode-locked Nd:YAG lasers [3], CO2 lasers operating at λ = 10 µm [4] and GaAlAs laser diodes operating at 0.85 µm, recently trying diode-pumped Nd:YAG lasers (λ = 1.06 µm) [5] and telecom InGaAsP semiconductor lasers operating at λ = 1.5 µm.

Advances in lasers, detectors, sensors, optics, and electronics have resulted in several successful ground-to-satellite/satellite-to-ground and inter-satellite communication demonstrations of optical systems [6]-[12]. These demonstrations involving laser communication (lasercom) links are summarized in **Table 1**, where the space terminals have been on near-Earth orbiting platforms. Advances in lasers, detectors, sensors, optics, and electronics have led to several successful ground-to-satellite/satellite-to-ground and inter-satellite communication demonstrations. These include optical links to spacecraft in Geosynchronous Transfer Orbit (GTO), Low-Earth Orbit (LEO) and Geostationary-Earth Orbit (GEO) to a Optical Ground Station (OGS) or another aircraft. Among these demonstrations, three Space to Ground scenarios have been identified, shown in **Figure 3**, with different link distance and target data rates [13].

***Table 1**: Successful OCW demonstrations for space*

Year	Project	Link	Rate (Gb/s)	Note
1995	LCE	GTO-to-Ground	0.001	JAXA
2001	GeoLITE	GEO-to-Ground	>1	USA
2001	SILEX	LEO-GEO	0.05	ESA
2002	ALEX	GEO-Air	>1	USA
2005	LUCE	LEO-GEO LEO-Ground	0.05	JAXA
2006	LOLA	GEO-Aircraft	0.05	France
2008	LCTSX	LEO-LEO	5.6	Germany

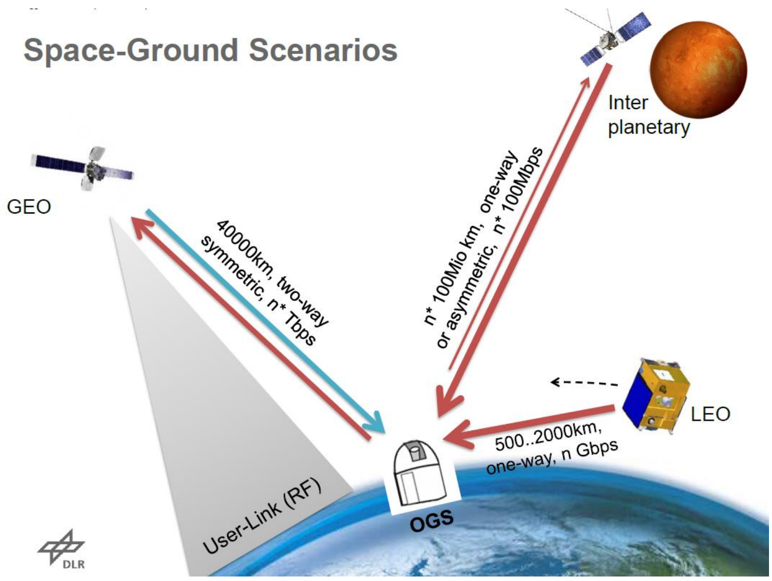

Figure 3: Space to ground optical communication scenarios[13].

2.2. OWC advantages

Free Space Optical Communications have several advantages over Radio-Frequency links. The most important of them are:

- **Increased Bandwidth**: It is a well-known fact that an increase in carrier frequency allows to increase the information carrying capacity (bandwidth) of a communication link. In RF communications, the allowable bandwidth can be up to 20% of the carrier frequency. For the Ka-band, where the center frequency is 24,3 GHz, means a maximum bandwidth of about 5 GHz. In an optical link, even if the bandwidth is taken to be 1% of carrier frequency (≈ 193 THz), the allowable bandwidth will be 1000 GHz, which is 200 times that of a typical RF carrier [2].

- **Reduced transmitted power**: The diffraction limited divergence angle is proportional to λ/D, where λ is the carrier wavelength and D the aperture diameter. Therefore, the beam spread of an optical carrier is narrower than that of the RF as shown in **¡Error! No se encuentra el origen de la referencia.** , depicting the comparison of beam divergence for optical and RF signals when sent back from Mars towards Earth. The power at the receiver is determined by the following expression:

$$P_{Rx} \approx \left(\frac{D_{Tx} \cdot D_{Rx}}{\lambda \cdot L}\right)^2 P_{Tx}$$

  This shows that the power at the receiver increases with $1/\lambda^2$. This leads to an increase in the intensity of signal at the receiver for a given transmitted power.

- **Reduction of antenna size (and mass):** Smaller wavelengths allow smaller antennas. As the antenna gain scales inversely proportional to the square of the wavelength, optical systems use smaller antennas than RF system to achieve the same gain. The typical size for the optical system is 0.3 m against 1.5 m for RF spacecraft antenna [14].

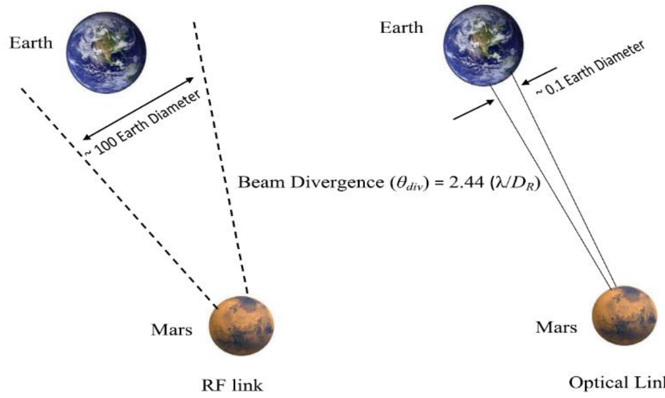

Figure 4: *Comparison between an RF and optical beam divergence from Mars towards Earth.*

Optics, with shorter wavelengths can project the transmitter power into a smaller area at the receiver, allowing much higher data rates. Because RF wavelengths are longer, the size of their transmission beam covers a wider area (about 160 km); therefore, capture antennas for RF data transmissions must be very large. Laser wavelengths are 10,000 times shorter, allowing data to be transmitted across narrower, tighter beams. The smaller wavelengths of laser-based communications are more secure, delivering the same amount of signal power to much smaller collecting antennas.

- **Unlicensed spectrum**: In the RF system, interference from adjacent carrier is the major problem due to spectrum congestion. This requires the need of spectrum licensing by regulatory authorities. But on the other hand, the optical system is free from spectrum licensing till now. This reduces the initial set up cost and development time.

Laser space communications are expected to provide significant reduction in antenna size applies for both ground and space receivers, which reduces satellite size and mass. Laser communication terminals can support higher data rates with lower mass, volume and power requirements, a cost savings for future missions.

2.3. OWC challenges

Free Space Optical Communications have several advantages over Radio-Frequency links. The challenges for OWC in ground-to-satellite and satellite-to-ground communications are mainly derived from the atmospheric effects. Within these scenarios, the relevant OCW uses the atmosphere as propagation channel, whose properties are a random function of space and time. Relevant effects to optical propagation appear within the first 17 km of the atmosphere, between the earth surface and the Tropopause, as shown in **Figure 5**. Above the Tropopause, the air ceases to cool with height and becomes almost completely dry. Those first 17 km of the atmosphere are responsible for making OWC a random phenomenon that is dependent on weather and geographical location.

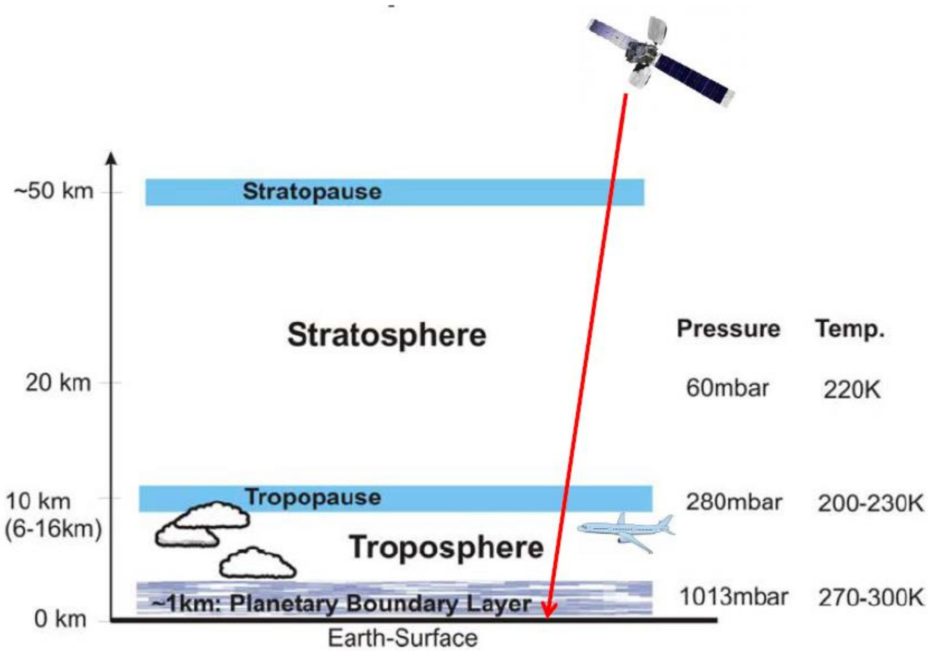

Figure 5: *Structure of the earth atmosphere [13].*

The most important challenges for the propagation of optical beams through the atmosphere within this region:

- **Propagation attenuation**: One of the effects of the atmosphere on optical signals is their attenuation by scattering (caused by clouds and molecules) and absorption (by molecular absorption lines matching the energy of the photons) phenomena. The following figure presents the attenuation coefficient per unit length of the atmosphere at different altitudes, highlighting the transmission windows at wavelengths where mature optical components from fiber communications exist. In addition to this, we must take into account that clouds and fog completely block optical links.

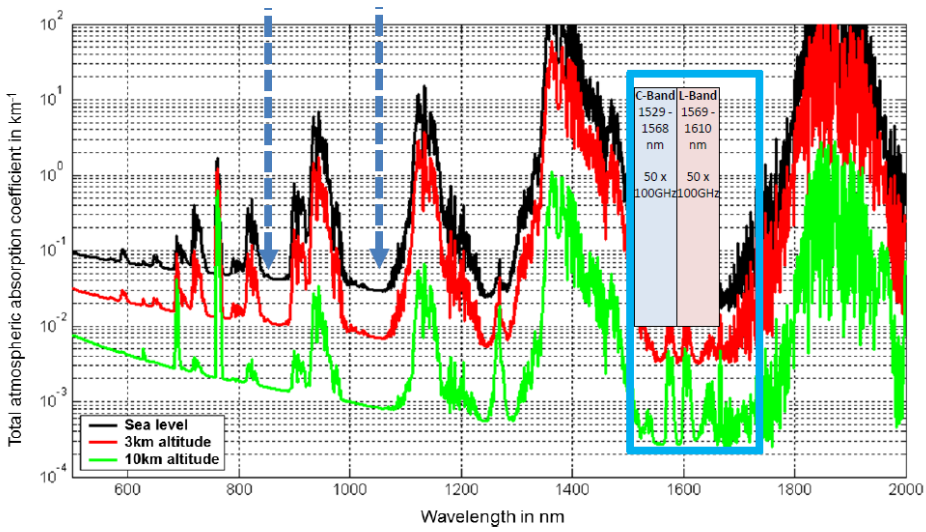

Figure 6: Atmospheric attenuation at infrared laser wavelengths [13].

- **Signal scintillation and beam wandering by index-of-refraction turbulence (IRT):** Signal scintillation is the variation in apparent brightness or position of a distant luminous object viewed through a medium. As shown in **Figure 7**, is the result of the interaction between the optical beam propagating through inhomogeneous air (caused by small-scale fluctuations in air density usually related to temperature gradients), resulting in intensity speckles and wave front distortions.
  A quantitative measure of the intensity of optical turbulence is the refractive index structure parameter, C_n^2, where averaged C_n^2 is often determined as a function of local differences in temperature, moisture, and wind velocity at discrete points.

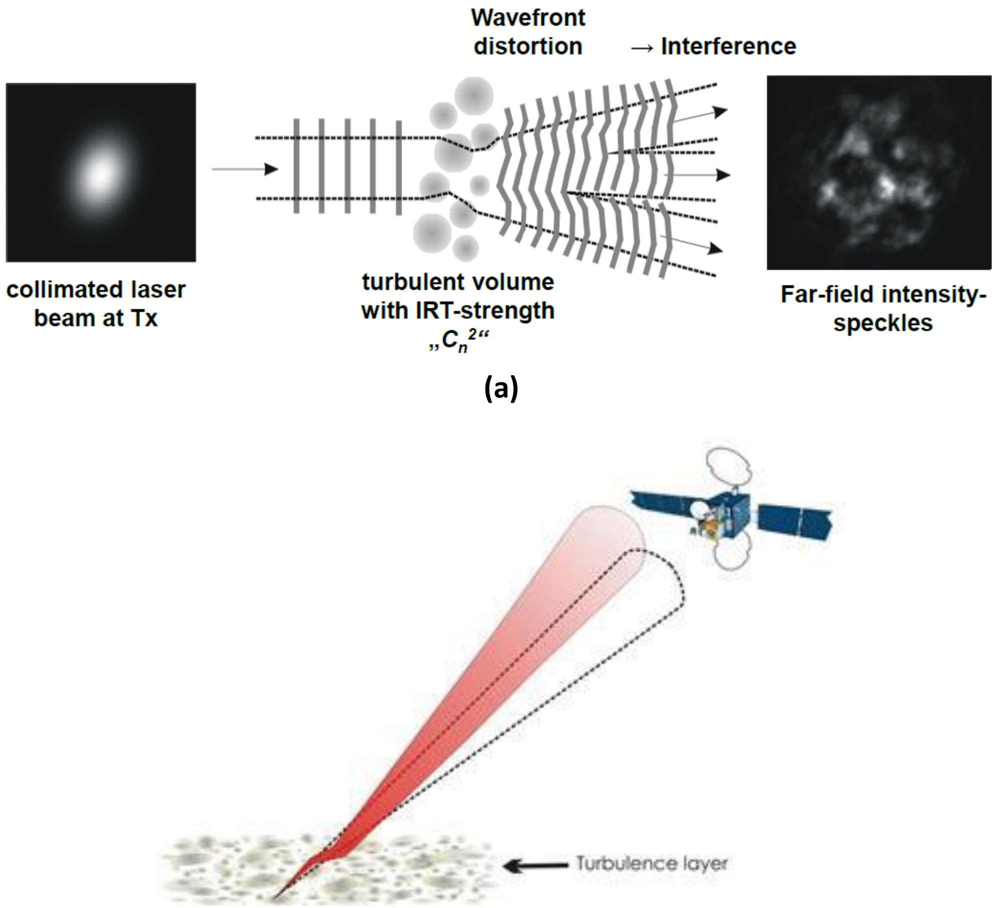

(a)

(b)

Figure 7: (a) Optical beam scintillation phenomena at turbulent layers of the atmosphere, and (b) resulting fading suffered by the satellite [13].

- **Precise pointing and tracking (link acquisition).**

For inter-satellite OWC links, various limiting factors include pointing, background noise and link availability [15].

2.4. Space laser terminal components

The block diagram of a full duplex terminal for space optical communications is represented in **Figure 8**, showing the different sub-systems involved.

The whole structure must be mounted on a **Coarse Pointing Assembly (CPA)** Mechanism, a high precision opto-mechanical pointing device. Different solutions have been used, being the most common an azimuth-elevation gimbal. This solution involves two actuator stages arranged at 90° angle to each other, each carrying a flat mirror mounted at 45° with respect to its axis of rotation. With this arrangement, each mirror deflects the optical beam by 90° effectively resulting in a full hemispherical pointing range. Other alternatives are a periscope or one-mirror structures.

The terminal mounted on the CPA has the telescope focus optics, which is the optical port for transmission and reception. The receiver chain includes several beam-splitters to illuminate key sub-systems that maintain the alignment between the satellite and the ground station. These may include an index-of-refraction turbulence (IRT) measurement devices (like DIMM, differential image motion monitor, a standard instrument in astronomy), a pupil camera (for measurements of the intensity distribution in the pupil plane), the tracking camera, a power meter, and Receiver Front-End (RFE).

As shown, the full duplex characteristic is achieved using two different wavelengths, one for the transmission direction (λ_B) and another for the reception (λ_A).

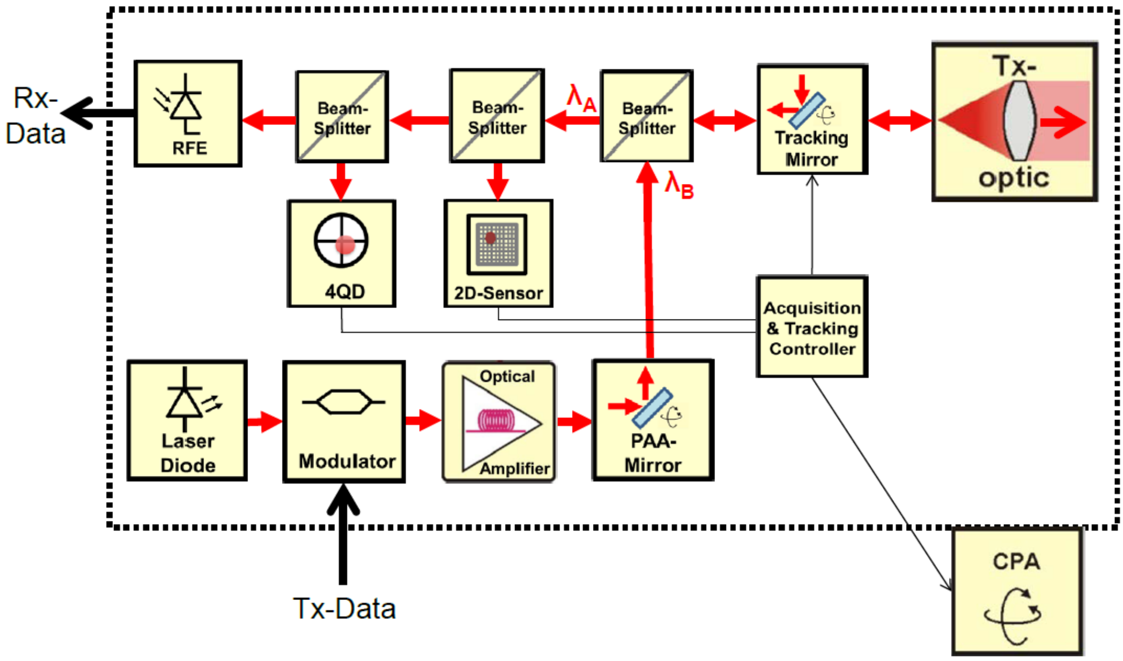

Figure 8: Components of full-duplex Space Laser Terminal

2.4.1 On-board terminals

As example of full-duplex laser terminals, first for **on-board terminals,** we include the description of the **VABENE terminal**, developed by the DLR Optical Communications Group in the Institute of Communications and Navigation, for an aeronautic laser downlink for real-time traffic and mass-events observation. This project established an optical link between a ground station and a Do-228 aircraft, which helped to optimize parameters of the laser link under the effects of the atmosphere and the platform vibrations. The characteristics achieved in this experiment were:

- The Coarse Pointing Assembly were located outside the aircraft, while the fine-pointing assembly and electronics were located inside.
- Mass of 60 kg, and power consumption of 70 W
- Maximum data rate, 1,25 Gb/s
- Maximum link distance of 150 km
- Laser wavelengths located within the C-band (1,45 to 1,6 µm)

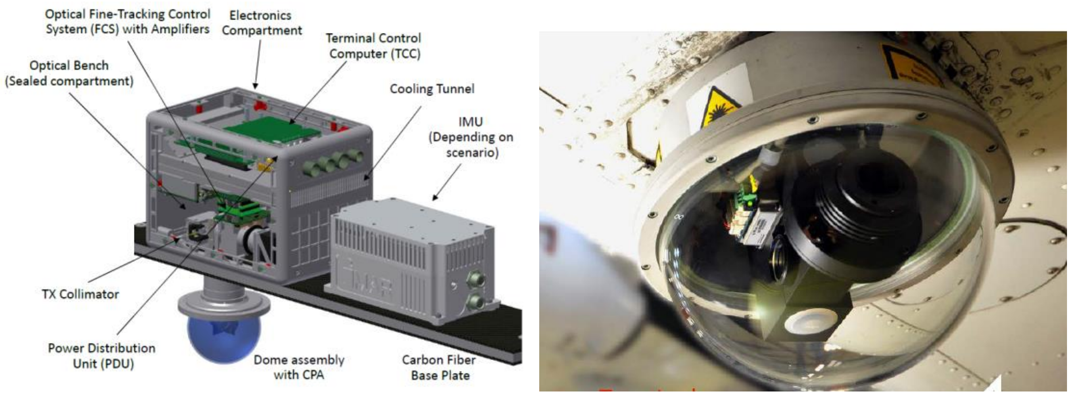

(a) (b)

Figure 9: (a) Elements in an on-board optical communications terminal, and (b) photograph of VABENE CPA attached to Do-228 aircraft

Another example of on-board system by the DLR Optical Communications Group is the **ViaLight** inter-platform link terminal, developed within CAPANINA European FP6 project. The characteristics of this system were:

- The Coarse Pointing Assembly (Az. 360º continuous, Elevation -19º to 90º). Fine-pointing system (1.9º, 2-axes).
- Mass of 3 kg for stratospheric vehicle, 15 kg. for airship, and power consumption of 80 W, at 28 V.
- Variable data rates, 10, 100, 1000 Mb/s. Telemetry and control, through a serial interface at 9.6 kb/s.
- Laser wavelengths located within the C-band (1,45 to 1,6 µm) and < 50 µrad divergence.

2.4.2 Ground Stations

For the first European laser communication system demonstration, done in the 1980s,. The ESA Optical Ground Station (OGS) was located in Tenerife (Canary Islands - Spain), at 2.400 meters of altitude, in the Teide Observatory. It took place within the Semiconductor Laser Intersatellite Link Experiment (SILEX) initiative, to connect with the ESA satellite Artemis. A 1-m Cassegrain Telescope shown in **Figure 10** was used. ARTEMIS satellite relayed in 2001 the first image from the LEO Satellite SPOT-4 to Earth [16] and since then has demonstrated successfully direct bidirectional links to the ESA OGS in Tenerife.

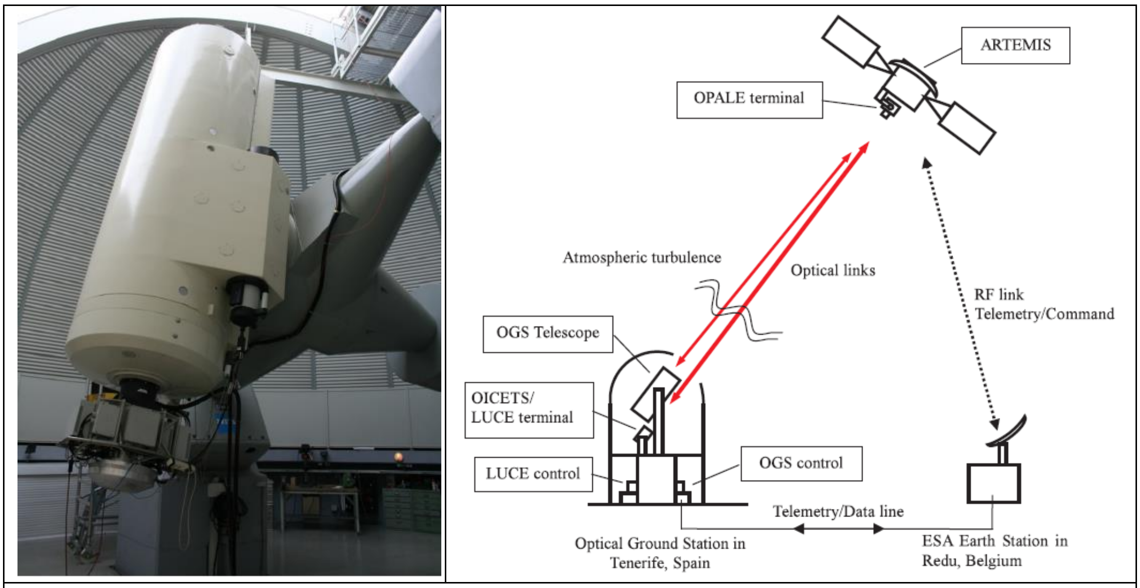

Figure 10: ESA Optical Ground Station (OGS) at Izaña peak, in the Teide Observatory astronomic complex, and setup of the optical satellite-to-ground link.

More recently, in 2006 and 2009, experiments to investigate the optical LEO downlink channel and evaluate the feasibility of optical transmission technology for future applications were conducted using the Japan Aerospace Exploration Agency (JAXA) Optical Inter-orbit Communications Engineering Test Satellite (OICETS, also called "Kirari"), a low earth orbit satellite. The optical detector mounted on OICETS can receive laser beams from two or more ground stations in different locations on the earth, a characteristic that could be used to clarify the difference in the atmospheric fluctuations in the different locations of ground stations by comparing the characteristics of the signals received from the stations. In order to carry this experiment, optical communication links were established between OICETS and different OGS in different parts of the world belonging to the German Aerospace Center (DLR), European Space Agency (ESA), Jet Propulsion Laboratory of the National Aeronautics and Space Administration (JPL/ NASA), and National Institute of Information and Communications Technology (NICT). The locations, latitudes, longitudes, and heights above sea level of the ground stations of these agencies are shown in **Table 2**.

Table 2: Comparison of location conditions of optical ground station

Organization	Location	Latitude	Longitude	Altitude
DLR	Oberpfaffenhofen	48.08° N	11.27° E	645 m
ESA	Tenerife Island	28.30° N	16.51° W	2,393 m
JPL	Table Mountain	34.38° N	117.66° W	2,200 m
NICT	Koganei	35.71° N	139.49° E	122 m

Every station is located between the latitudes 28° and 48° in the northern hemisphere. The DLR ground station is located on the European Continent and can be used for experiments at a relatively-low elevation angle (of several degrees). The other stations are all located near the ocean. The ESA and JPL stations are located more than 2,000 m above sea level, where low atmospheric fluctuations are expected. The elevation angle of the satellite in the experiments, although it varies depend ing on the orientation at the start of the experiments, was 0° for the DLR and ESA stations, 20° for the JPL station, and 15° for the NICT station.

In this experiment, the Institute of Communications and Navigation (IKN) of the German Aerospace Center (DLR) used an Optical Ground Station located at Oberpfaffenhofen, near Munich, shown in **Figure 11**. It comprises several devices for measuring the effect of the atmosphere's index-of-refraction turbulence (IRT) and a data receiver frontend to quantify bit-error distributions. This project was named KIODO (KIrari Optical Downlinks to Oberpfaffenhofen). The optical receiver was based on a Cassegrain Reflecting Telescope with 40 cm aperture diameter sheltered in a fully opening clam-shell dome to allow tracking of objects with fast azimuth velocity. The optical transmitter was based on a 10 W laser beam with beam divergence angle of 5 milliradian. The optical receiver was based on an Avalanche Photo-Diode (APD).

For the first campaign in summer 2006, the telescope's focus optics was fitted with several beam-splitters to illuminate different index-of-refraction turbulence (IRT) measurement devices like DIMM (differential image motion monitor, to measure the Fried-parameter), a pupil camera (for measurements of the intensity distribution in the pupil plane), the tracking camera, a power meter, and the data receiver frontend. Furthermore, a separate 5 cm refractor telescope was also used for power measurements, which is useful to compare aperture averaging influence of small to large receiver apertures. For the second campaign, in 2009, a focal spot camera, a high-speed data logger for the received analog data signal, and a Shack-Hartmann wavefront sensor (SHWFS) were added.

Optical link trials were attempted at night, each one at approximately the same local time. Viewed from the ground station, satellite passes have different maximum elevation angles. The operation of the "Laser Utilizing Communications Equipment" (LUCE) optical terminal onboard OICETS, had some constraints regarding its angular speed and the position of the Sun with respect to its field of view. Due to these constraints, each trial was limited to a predetermined pass segment and a corresponding elevation span.

After these experiments, it was concluded that the combination of four OSG helps to download massive data from space with the probability of 99%. The statistics of NICT for the establishment of the link (which achieved a 49%probability of success) are shown in **Figure 12**.

Figure 11: (a) DLR Optical Ground Station (OGS) dome at Oberpfaffenhofen, and (b) View of the focal bench of the 40-cm telescope.

***Table 3**: Overview of the KIODO trials Table 4 in 2009.*

KIODO Trial	Day of June 2006	Time (UTC) of Pass Start	Maximum Pass Elevation	Measurement Elevation Span	Weather	Remark
KT06-1	7^{th}	1:13	45.5°	10–35°	90% clear sky, 8°C	No scintillation / DIMM measurement
KT06-2	9^{th}	0:02	33.5°	10–32°	90% clear sky, 10°C	No BER measurement
KT06-3	14^{th}	1:04	55.6°	10–45°	clear sky, 10°C	
KT06-4	15^{th}	23:54	28.0°	2–27°	80% clear sky, 12°C	
KT06-5	21^{st}	0:56	68.2°		Cloudy	No Link
KT06-6	23^{rd}	1:21	38.4°		Cloudy	No Link
KT06-7	28^{th}	0:47	83.2°	4–43°	Thunder clouds 1 h before trial, 18°C	
KT06-8	30^{th}	1:12	46.5°		Cloudy	No Link

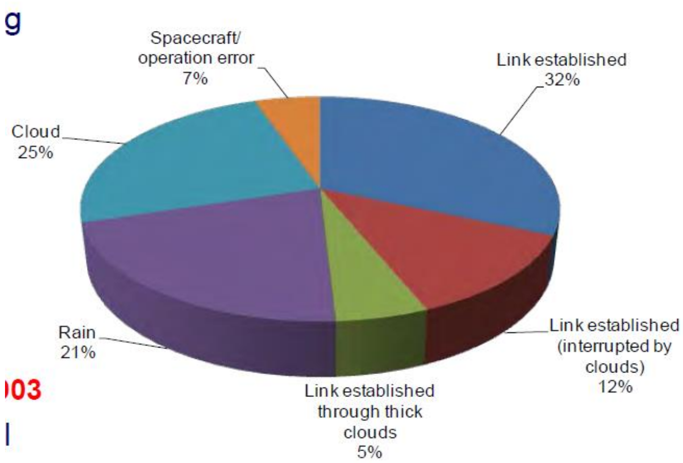

Figure 12: Statistics of link establishment at NICT

3. Major space agency's efforts towards OWC

3.1. NASA

NASA took the lead in 2013 with the Lunar Laser Communications Demonstration (LLCD), which successfully demonstrated optical communications in space. The LLCD returned data from the **Lunar Atmosphere Dust Environment Explorer (LADEE) spacecraft** to earth with an optical laser link at a record speed of 622 Mbps, capable of streaming more than 30 HDTV channels simultaneously [18]. Data is transmitted in the form of short light pulses, sent by the **Lunar Lasercomm Space Terminal (LLST)**, aboard the LADEE spacecraft.

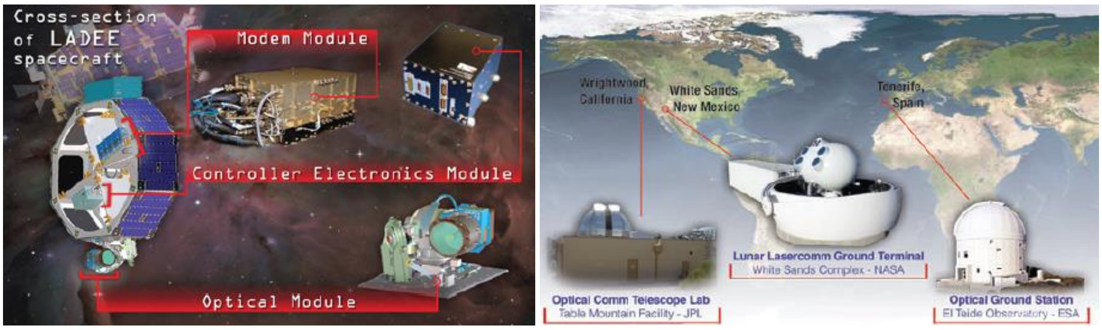

(a) (b)

Figure 13: (a)LADEE modules, and (b) LLCD ground terminals

The LADEE data transmissions are downlinked to one of the three ground telescopes in New Mexico, California or Spain. The LLST, developed by the Massachusetts Institute of Technology's (MIT) Lincoln Laboratory in Lexington, Mass., is comprised of three modules: the optical module, the modem module and the controller electronics module. The entire system weighs about 30 kilograms. The optical module is mounted to the exterior of the LADEE spacecraft and consists of a 165-cm diameter telescope on a two-axis gimbal. This position allows LLCD to precisely point its laser beam back to Earth over a variety of spacecraft orientations. The modem is mounted inside LADEE and contains the 0.5-watt infrared laser transmitter that will transmit data at a rate of 622 Mbps from the Moon to Earth. The modem also contains the highly sensitive receiver that deciphers the light pulses of data sent from the ground telescopes at up to 20 Mbps. The optical module telescope transmits and collects the signals transmitted to and from Earth to the modem module by fiber optic cables.

Currently, NASA has continued to expand its optical communications program since the success of the Lunar Laser Communications Demonstration (LLCD). The next mission is the **Laser Communications Relay Demonstration** (LCRD)[19], shown in **Figure 14** designed to complement and possibly supersede RF single access (SA) service at Ka-band on the next generation of NASA's near-Earth relays. LCDR is developing Optical Space Terminals (OSTs) providing a bi-directional optical link encoding data onto a beam of laser light, with higher-bandwidth duplex data links to ground or low-Earth orbit (LEO) users of up to 2.88 Gbps un-coded or 1.244 Gbps with ½ rate DVB-S2-based FEC.

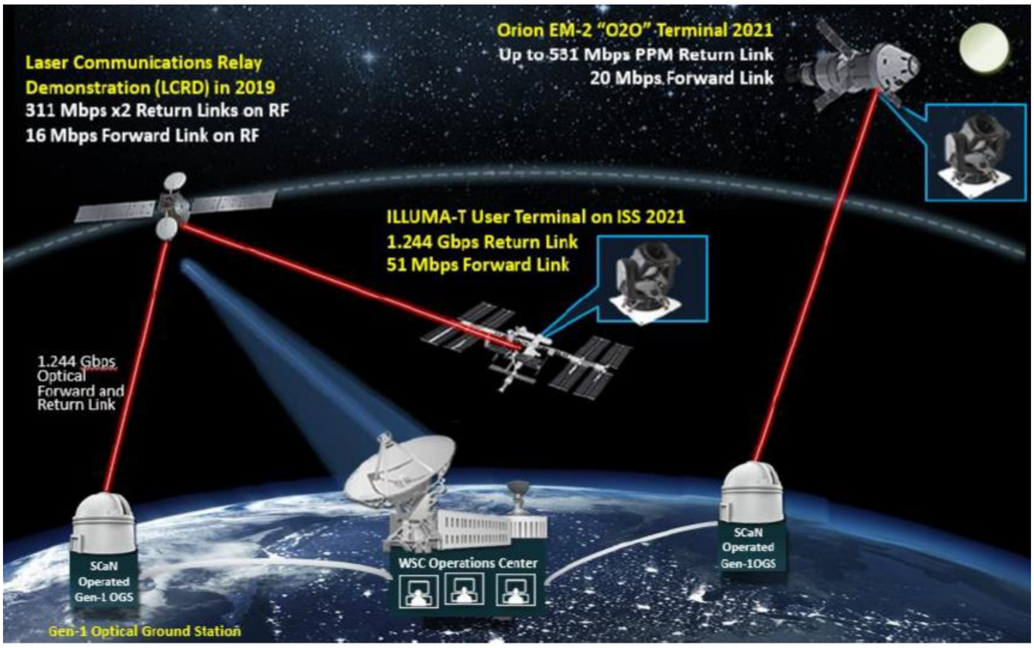

Figure 14: (a) NASA's near-term missions for near-Earth optical communications 2019-2021 [19].

For LCRD to provide similar services, a user terminal is required to close LEO-GEO links of 40,000 km or longer. NASA SCaN is developing the **Integrated Lasercomm LEO User Modem Amplifier – Terminal** (ILLUMA-T) for such users, with an initial demonstration from the International Space Station (ISS) in early 2021. It will be based on a new 10 cm optical module known as the **Next Gen Terminal (NGT)**, which will again be controlled by a variant of the LCRD-based COTS Controller Electronics (CE). ILLUMA-T also includes a new, commercially-available 2.88 Gbps DPSK modem, which includes an erbium-doped highpower optical amplifier (HPOA) which can transmit up to 3 W at 1550 nm both as a beacon and for communications. The NGT uses a 2-axis gimbal but unlike the OM for LCRD, it can articulate over a large field-of-regard (360° azimuthal x 270° elevation) to allow for communications independent of the spacecraft bus orientation. It is also designed to provide fine pointing and tracking at the high gimbal slew rates required for LEO-GEO or even LEO-GND tracking.

3.2. ESA

In summer 1977, ESA placed a technological research contract for the assessment of modulators for high-data- rate laser links in space. This marked the beginning of a long and sustained ESA involvement in space optical communications. A large number of study contracts and preparatory hardware development followed, conducted under various ESA R&D and support technology programmes. In the mid- 1980's, ESA took an ambitious step by embarking on the SILEX (Semiconductor laser Intersatellite Link Experiment) programme, to demonstrate a pre-operational optical link in space, between a terminal embarked on the French LEO observation satellite SPOT4 (launched on 22nd March 1998) and a terminal embarked on ESA's GEO telecommunication satellite ARTEMIS (launched on 12th July 2001). ESA achieved the world premiere demonstrating the first laser link between these two satellites on 22nd November 2001 [20].

Figure 15: ESA world demonstration the first laser link between Artemis and SPOT4 on 22nd November 2001 communicating via SILEX.

SILEX was a free-space optical communication system which consists of two optical communication payloads to be embarked on the ESA Artemis (Advanced Relay and TEchnology MIssion Satellite) spacecraft and on the French Earth-observation spacecraft SPOT-4, allowing data transmission at 50Mbps from low Earth orbit (LEO) to geostationary orbit (GEO) using **GaAlAs laser-diodes and direct detection**.

ESA achieved again a milestone in Spacecraft Engineering by the introduction of fiber optic technology. The dual launch of SMOS (carrying over 700m optical communication links for its payload, the biggest in the world) and PROBA II (carrying the first fiber optic sensor subsystem in the world) in November 2009 mark the starting point for Photonics Space Flight in European Space Missions.

The first satellite to extensively use fiber optics for its main Payload (P/L) was ESA's SMOS satellite launched in November 2009. Within the same launch ESA's PROBA II technology demonstration satellite carried the first fiber optic sensor system, instrumenting the S/C's propulsion subsystem. Both operate flawlessly after 8 years demonstrating the usefulness and robustness of the technology and serve as a baseline example for more advanced use of photonics in the spacecraft (S/C) and payload (P/L).

Since then, and driven by the requirements of the Telecommunication satellites for High Throughput Payloads, photonic technologies have emerged as an enabling technology in COMSATs. In Analog Payloads hybrid microwave/photonic designs have been proposed by the two main primes which plan to offer this solution to RFQ by Operators as soon as 2019/20. Similarly, for the Digital Payloads, high-speed optical have been baselined for first time in 2017 by one of the big Primes (links at rates up to 20 Gbps) while the requirement for the next generation Digital Payloads calls for 56 Gbps data rates.

For the Satellite Platforms, fiber optics are currently under development and qualification for use as the thermal monitoring subsystem. Also, novel approaches for incorporating such a fiber optics-based thermal monitoring subsystem in pre-fabricated S/C panels lead to a new paradigm on how to build a S/C in a shorter Assembly Integration and Testing time. On the communication cabling linking the various instruments to the On-Board Processor or Mass Memory the “Space-Fiber” has been established and it is now going through ECSS standardisation. This process will promote the fiber-based “Space-Fiber” as eventually the preferred standard and medium for the communications links with instrumentation.

3.3. JAXA

Research in optical communications in space in Japan have been performed since the 1980s at various research institutes and universities, among them the National Institute of Information and Communications Technology (NICT), Advanced Telecommunications Research Institute International (ATR) and Japan Aerospace Exploration Agency (JAXA) [21]. In 1994, laser communication equipment (LCE) developed by NICT was mounted on the JAXA engineering test satellite Ⅵ and was successfully used for communications between a satellite and the ground for the first time in the world [22].

After this successful demonstration, the Optical Inter-orbit Communications Engineering Test Satellite (OICETS, known as “Kirari”) was developed, mostly for two purposes. The first one, to conduct experiments of optical inter-orbit communications between a low earth orbit and a stationary orbit, using OICETS and stationary satellite ARTEMIS developed by the European Space Agency (ESA). The second, to perform experiments of optical communications between low earth orbit and the ground using OICETS and the NICT optical ground station. OICETS was deployed in August 2005 into a sun synchronous orbit of an altitude of about 610 km and an orbital inclination of 97.8°.

Each of JAXA OICETS and ESA ARTEMIS have originally-developed optical inter-orbit communications equipment. To conduct communications experiments in orbit, JAXA and ESA jointly created the **Space Segment Interface Document (S-ICD)** to share communications interface specifications, and each of them developed optical inter-orbit communications equipment according to these specifications. S-ICD specifies the wave length, modulation method, intensity, pulse characteristics of optical modulating waves, and sequence of tracking and pointing each other’s laser beams, etc. The major interface rules of S-ICD are shown in **Table 4**.

The optical inter-orbit communications equipment mounted on the OICETS is called LUCE (Laser Utilizing Communication Equipment) and that on the ARTEMIS is called OPALE (Optical Payload Laser Experiment). The significant functional difference between LUCE and OPALE is the presence/absence of a beacon light transmission unit.

Beacon light is used only at the initial stage of the tracking and pointing sequence. A beacon beam of a spread angle of 750 µrad, wider than the spread angle of 6 µrad of communications laser beams, is radiated to the target satellite. By scanning it in a spiral form, important initial tracking can be secured.

***Table 4**: Major rules of interface for optical inter-orbit communications*

	Forward link (OPALE to LUCE)	Return link (LUCE to OPALE)
Wavelength	819nm (communication beam) 801nm (beacon beam)	847nm (communication beam)
Polarization	LHCP	LHCP
Data rate	2.048M bps	49.3724M bps
Modulation	IM-DD	IM-DD
Signal format	2PPM	NRZ
Extinction Ratio	$< 2\%$ Imin/Imax	$< 2\%$ Imin/Imax
Intensity	Min. 25.2MW/sr Max. 130MW/sr	Min. 280MW/sr Max. 780MW/sr
Bit error rate	$< 10^{-6}$	$< 10^{-6}$

3.4. CNSA

China has been working over more than ten years developing a sophisticated satellite, Micius. A cross-disciplinary, multi-institutional team of researchers from the Chinese Academy of Sciences, led by professor Jian-Wei Pan have developed this satellite for quantum science experiments. Is was launched on August 2016 and orbits at an altitude of ~500 km (310 mi). In this satellite, optical links are established for Quantum Key Distribution (QKD), having developed single-photon detectors that can operate in space.

For this satellite, China has built five ground stations to cooperate with the Micius satellite, located in Xinglong (near Beijing), Nanshan (near Urumqi), Delingha, Lijiang and Ngari in Tibet.

4. Space qualification of photonic components

Traditionally, the development of optical communication systems has been developed with discrete components. The photonic components used in photonic payloads come from terrestrial networks applications, but this raised the problem of their ability to withstand space environment[23].

The **Qualification Process** is critical for any technology that challenges the existing ones unless there is immediate need. Photonic is not an exemption to this general rule. Today we have relatively few photonic parts in the European QPL list, and there is little motivation to qualify parts for space as the market is seen as being very small. Establishing a comprehensive roadmap for European industry will go some way to persuading industry to invest in making products designed for the space environment.

As the technology becomes more widely used across the industry it will be important to identify standards to cover the procurement, testing and evaluation of these devices to permit wider use of the technology. To this end there exists a lack of ESCC standards for the evaluation and qualification of optical components for space.

A first step in the qualification of optical components has addressed optical intensity modulators, identified as key components to perform functions such as generation and distribution of optical local oscillators or optical mixing in future telecommunication payloads. Several technologies are commercially available exhibiting different levels of performance and maturity for space applications.

The assessment of optical modulators was done using modulators from different suppliers and covering these different technologies, procuring the components and submitting them to a full test campaign encompassing functional as well as environmental tests. Among them, lithium niobate and semiconductor electro-optical modulators turn out able to withstand most of environmental tests while keeping good overall performances and so appear as the best technologies for space applications at 1.55 µm.

5. Future trends

Within photonics technology, there is a current effort in the development of photonic integration [24]. Photonic integrated circuits are the chip scale integration of multiple optical elements or components which enable complex functions analogous to the electrical integrated chips. As these chips increase in complexity and functionality they are finding new space applications (laser beam steering, complex optical modulation/demodulation, optical switching, optical beam forming, packet processing). The main advantage of this approach is to decrease size and weight, but also a reduction in power consumption. The main drawback is the limited amount of optical power delivered by photonic integrated circuit components. As an example, a novel structure for monolithically integrated tunable semiconductor lasers produce a laser beam with an optical linewidth of 363 kHz, delivering up to 3 mW output power, with a record tuning range of 74.3 nm. Thus, a way to boost the optical power delivered by photonic integrated circuits must be provided.

References

[1] D. Powell “Lasers boost space communications” Nature (2013).

[2] W. D. Williams et al., “RF and optical communications: A comparison of high data rate returns from deep space in the 2020 timeframe,” Glenn Res. Center Cleveland, Ohio and NASA Center AeroSp. Inf., Nat. Aeronautics Space Admin., Tech. Rep. NASA/TM-2007-214459, 2007.

[3] M. Ross, P. Freedman, J. Abernathy, G. Matassov, J. Wolf, J. D. Barry: Proc. IEEE 66 (1978) 319.

[4] J. H. McElroy, N. McAvoy, E. H. Johnson, J. J. Degnan, F. E. Goodwin. D. M. Henderson, T. A. Nussmeier, L. S. Stokes, B. J. Peyton, T. Flattau: Proc. IEEE 65 (1977) 221.

[5] K. Pribil, Ch. Serbe, B. Wandernoth, Ch. Rapp: Proc. Free-Space Laser Communication Technologies VII, 1995 (SPIE Vol. 2381) p.83.

[6] K. L. Sterckx, J. M. H. Elmirghani, and R. A. Cryan, “Pyramidal fly-eye detection antenna for optical wireless systems,” Opt. Wirel. Commun. (Ref. No. 1999/128), IEE Colloq., no. i, p. 5/1-5/6, 1999.

[7] K. E. Wilson and J. R. Lesh, “Overview of the ground-to-orbit lasercom demonstration”, Proc. SPIE Free-Space Laser Commun. Technol. IX, vol. 2990, pp. 1–9, Jan. 1997.

[8] J. Keller “Optical links are key to next-generation military communications satellites”, Military Aerosp. Electron., vol. 15, no. 4, Apr. 1, 2004. Available: http://mae.pennnet.com/articles/article_display.cfm?article_id=202216.

[9] T. Tolkeer-Nielsen and G. Oppenhauser, “In-orbit test results of an operational intersatellite link between ARTEMIS and SPOT4”, Proc. SPIE Free-Space Laser Commun. Technol. IX, vol. 3615, pp. 31–42, Apr. 1999.

[10] H. Hemmati, Ed., “Near-Earth Laser Communications”. CRC Press (Boca Raton, FL 2009), p. 24.

[11] M. Toyoshima et al., “Results from phase-1, phase-2 and phase-3 kirari optical communication demonstration experiments with the NICT optical ground station (KODEN), in Proc. 25th AIAA Int. Commun. Satellite Syst. Conf., 2007, AIAA 2007-3228.

[12] L. Vaillon, G. Planche, V. Chorvilli, and L. Le Hors, “Optical communications between an aircraft and a GEO relay satellite: Design & flight results of the LOLA demonstrator,” in Proc. 7th Int. Conf. Space Opt., 2008.

[13] D. Giggenbach "Optical Free Space Links for Satellite-Ground Communications” 7th Advanced Satellite Multimedia Systems Conference, Livorno (2014)

[14] A. K. Majumdar and J. C. Ricklin, “Free-Space Laser Communications: Principles and Advances”, vol. 2. New York, NY, USA: Springer, 2008.

[15] H. Kaushal and G. Kaddoum, “Optical Communication in Space: Challenges and Mitigation Techniques,” *IEEE Communications Surveys & Tutorials*, vol. 19, no. 1, pp. 57-96, First Quarter 2017.

[16] T. Tolker-Nielsen and G. Oppenhauser. In-orbit test result of an operational optical intersatellite link between artemis and spot4, silex. volume 4635, pages 1–15. SPIE, 2002

[17] D. Giggenbach, F. Moll, and N. Perlot "Optical Communication Experiments at DLR" Journal of the National Institute of Information and Communications Technology Vol. 59 Nos. 1/2 (2012).
[18] https://www.nasa.gov/sites/default/files/llcdfactsheet.final_.web_.pdf
[19] E. Luzhansky, B. Edwards, D. Israel, D. Cornwell, J. Staren, N. Cummings, T. Roberts, R. Patschke, "Overview and Status of the Laser Communication Relay Demonstration", *Proc. of SPIE*, vol. 9739, pp. 97390C-1.
[20] http://www.esa.int/Our_Activities/Telecommunications_Integrated_Applications/A_world_first_Data_transmission_between_European_satellites_using_laser_light
[21] M. Fujise, K. Araki, H. Arikawa, and Y. Furuhama, "Current and Future Activities in the Area of Optical Space Communications in Japan," Proceedings of SPIE, Vol. 1522, pp. 14–26, (1991).
[22] Y. Arimoto, H. Okazawa, M. Shikatani, T. Takahashi, M. Toyoda, M. Toyoshima, and K. Araki, "Laser communication experiment using ETS-VI satellite," CRL Journal, Vol. 42, No. 3, pp. 285–292 (Nov. 1995).
[23] A. Le Kernec, M. Sotom, B. Bénazet, J. Barbero, et al "Space evaluation of optical modulators for microwave photonic on-board applications" International Conference on Space Optics—ICSO 2010. Greece, 4–8 October 2010.
[24] https://www.esa.int/Our_Activities/Space_Engineering_Technology/Space_Optoelectronics/Photonics